MSUCL-207
March 1976

Shell-Model Calculations for the Zinc Isotopes*

J.F.A. van Hienen,** W. Chung and B. H. Wildenthal
Cyclotron Laboratory and Department of Physics
Michigan State University, East Lansing, Michigan 48824

ABSTRACT

Shell-model calculations for the zinc isotopes have been carried out with active particles distributed in the $1p_{3/2}$, $0f_{5/2}$ and $1p_{1/2}$ orbits outside a closed "^{56}Ni" core. The effective Hamiltonian used was one obtained by Koops and Glaudemans from a fit to Ni and Cu level energies. An average absolute deviation of 0.19 MeV between the calculated and experimental ground-state binding energies is obtained for the A=62-68 Zn isotopes. Good agreement is also found between most calculated and experimental excitation energies and spectroscopic factors for single-nucleon transfer for the low-lying levels in these nuclei. Experimentally known B(E2) values are generally well reproduced by the present model with effective charges of 1.0±0.1 and 1.6±0.2 for the neutron and proton, respectively. Magnetic dipole as well as Gamov-Teller transitions are not well accounted for by these calculations and seem to be sensitive to excitations of the ^{56}Ni core.

* Research supported in part by the U.S. National Science Foundation.
** Fellow of the Niels Stensen Foundation, The Netherlands.

1. Introduction

The aim of this study has been to develop a systematic description of the zinc isotopes (A=62-68) with shell-model wave functions. Despite the numerous experimental papers on zinc nuclei, only a few theoretical investigations have been devoted to them. In some of these previous theoretical studies the level structure of the even-A zinc nuclei has been described in terms of an anharmonic vibrator[1,2] and the structure of the low-lying levels in the odd mass nuclei explained[3] as the result of the coupling of the additional, odd particle to the vibrating core. An example of this type of theory, the "quasi-particle-phonon coupling model" of ref. [1], has been used in several experimental papers[4,5] on Zn nuclei in attempts to understand the measured decay schemes. However, these calculations are restricted to, and quite dependent upon, the specific properties of the described nucleus. A more general description of the nuclear properties of the zinc isotopes is given by Hartree-Fock-Bogoliubov calculations in the upper fp shell[6-9]. Here, an oblate shape of the ground states of the even zinc isotopes with A=62-68 has been found[6] and some inter-band E2 transition strengths calculated[9].

As far as shell-model calculations are concerned, a model in which the doubly closed ^{56}Ni nucleus acts as an inert core, with active particles distributed over the $1p_{3/2}$, $0f_{5/2}$ and $1p_{1/2}$ orbits, has been shown to be rather successful in describing the nuclear structure of the Ni and Cu isotopes[10-16]. At least for the lighter Zn isotopes it is very plausible that this same model

should yield comparable or even better results. However, no such calculations for Zn have been done previously, presumably at least in part because of the problems associated with the dimensions of the energy matrices. As a consequence of the developing experimental understanding of the Zn isotopes, the encouraging results of the shell-model studies on the Ni and Cu isotopes, and our development[17] of techniques to easily deal with the dimensionalities entailed, we have carried out the systematic shell-model study of the Zn isotopes described in the following.

The fundamental assumptions of the present work are that ^{56}Ni forms an inert core (no $0f_{7/2}$ excitations) and that the active particles are restricted to occupancy of the $1p_{3/2}$, $0f_{5/2}$ and $1p_{1/2}$ orbits. These assumptions affect the present calculations in various ways. As far as core excitation are concerned, only Hartree-Fock calculations[6-9] suggest that $f_{7/2}$ excitations are important for Zn. No firm experimental evidence of $f_{7/2}$ holes in the Zn ground states is found from stripping experiments,[18,19] however. It is assumed here that $f_{7/2}$ core excitation effects can be implicitly encompassed in the present model via effective two- and one-body operators. This approach has been applied with reasonable success in the case of similar calculations for Ni and Cu isotopes[10-16] with A=57-68.

The restriction of the present configuration space to the fp orbits is probably more important in that $0g_{9/2}$ particles are thereby excluded. There is evidence that $0g_{9/2}$ configurations exist in the ground states of ^{66}Zn and ^{68}Zn with particle occupation numbers of at least 0.7 and 0.9, respectively, from single-neutron

pick-up experiments[20,21], and the $g_{9/2}$ single-particle states are identified at low excitation energies in the odd-mass isotopes.

Pairs of $g_{9/2}$ nucleons coupled to J=0 can be seen theoretically to constitute important admixtures to the Zn wave functions when the large pairing energy in the $g_{9/2}$ orbit relative to the fp orbits is considered. This effect is demonstrated experimentally in the case of ^{71}Zn, where the ground state spin is $1/2^-$ and not $9/2^+$. It is none-the-less possible that the effects of $g_{9/2}$ activity in "fp-parity" states of the lighter Zn isotopes can also be largely subsumed into the fp wave functions via renormalization as is suggested by refs. [22] and [23] for A=58-60 Ni and Cu isotopes. Obviously, as the closure of the fp shell is approached this becomes more tenuous. The advantage of restricting the basis space to the three orbits considered lies in the fact that a single model, describable simply in terms of active orbits, with no further truncation procedures, is thus feasible to apply to a range of nuclei without further modification.

In the present work we have employed as the effective one-plus two-body Hamiltonian the one derived by Koops and Glaudemans[16] for the Ni and Cu isotopes. The single-particle energies are $E(p_{3/2})$ = -10.27 MeV, $E(f_{5/2})$ = -9.42 MeV, and $E(p_{1/2})$ = -9.05 MeV. The two-body part of this Hamiltonian consists of empirical modifications of surface delta (MSDI) two-body matrix elements[24] which were originally adjusted to best fit the energy levels of the Ni and Cu isotopes. The adjustments to the MSDI numbers yield slight improvements to calculated energy level spectra and single-nucleon spectroscopic factors for the Ni and Cu isotopes. Hence, this

work on Zn is a direct extension of the Glaudemans-Koops work on Ni and Cu, and can be considered in one context as an independent and thorough test of their Hamiltonian. It should be clear, of course, that a more efficacious Hamiltonian for Zn could have been obtained if Zn energy level data were also included in the data set by which the effective Hamiltonian matrix elements were determined. Our estimation was, however, that such changes were unlikely to substantively improve the quality of the wave functions of the Zn levels, and we have preferred the simpler and more direct approach of exactly extrapolating the Ni-Cu results to Zn.

In the following sections we will compare the theoretical values of level energies, single-nucleon spectroscopic factors, electric-quadrupole and magnetic-dipole electromagnetic phenomena, and Gamow-Teller beta-decay rates with experimental data in order to determine how well a moderately complete shell-model such as considered here can account for the nuclear structure of the A≃60-67 region.

2. Binding Energies and Spectra

A first test of the results of the present calculation is a comparison of the calculated level schemes with the available experimental data on the Zn isotopes[25-33]. The experimental ground-state binding energies of the Zn isotopes with respect to the ^{56}Ni core have been taken from the values of ref. [34]. A first-order Coulomb energy correction to these binding energies has been obtained by subtracting the Coulomb displacement energies in Cu with respect to Ni and those in Zn with respect to Cu for

each mass number. These energies have been obtained from a fit to the experimental values of ref. [35]. This means that average two- as well as one-body effects in the Coulomb energy have been taken into account. No further Coulomb energy corrections have been applied to the excitation energies. The calculated ground-state binding energies of the A=62-68 nuclei have an average deviation of 0.19 MeV from the corrected experimental values. (If ^{60}Zn and ^{61}Zn are included in the comparison, the average deviation drops to 0.17 MeV.) The largest deviation appears at ^{68}Zn. But here, a $g_{9/2}$ single-particle strength of 0.9 has been found in the 0^+ ground state from a single-neutron pick-up experiment[21], and these growing admixtures cannot be taken into account in the A-independent Hamiltonian of the present calculation.

The calculated binding energies may be compared also with the results of the recent Hartree-Fock-Bogoliubov calculation (HFB) of ref. [9] in which a full 0f-1p configuration space outside a closed ^{40}Ca core was employed, together with Kuo-Brown two-body matrix elements. These results and the present ones are both shown in fig. 1 and compared with the experimental values for the Zn isotopes with A=61-68. In fig. 1, differences between ground-state binding energies of neighbouring nuclei are plotted as a function of the mass number. This comparison shows the good agreement with experiment of the present (ASDI) results as well as the large deviations calculated with the HFB method[9] when going from an even to an odd mass number. The latter effect is perhaps due to an inappropriate projection method, since the calculated quadrupole moment of the ground state in ^{63}Zn is opposite in sign to the experimental value.

Along with the spectra of excited states, the absolute values of the experimental (Coulomb corrected) and calculated (ASDI) ground-state binding energies of the Zn isotopes with respect to ^{56}Ni are shown in figs. 2 and 3. As regards excitation energies, the general features of the even-mass Zn nuclei are well described by the present calculations as shown in fig. 2. However, there are some instances in which the present model results clearly and rather consistently deviate from experiment. The most obvious problem occurs with the predicted values of the third 2^+ states, which are, except in ^{68}Zn, about 0.6 MeV too low compared to experiment. If the MSDI set of two-body matrix elements from ref. [16] is used, similar results are found, so this discrepancy may be a result of the configuration space limitations rather than the specification of the Hamiltonian.

Another discrepancy occurs for the first excited 0^+ states, which are correctly predicted in case of ^{62}Zn and ^{64}Zn, but are calculated too high for the other masses. However, in case of ^{68}Zn, one can expect that a configuration for this 0^+ state with two zero-coupled neutrons in the $g_{9/2}$ is energetically favored over one with a filled $1p_{1/2}$ or $0f_{5/2}$ neutron sub-shell, as is required in the present calculation. (Direct information about how the dominant components of the model wave functions agree with the experimentally observed properties of the corresponding state can be obtained from the single-nucleon-transfer spectroscopic factors, as will be discussed subsequently.)

The model predicts 3^+ states at what are perhaps surprisingly low energies. No 3^+ states are experimentally known. The

calculated energies of 1^+ states, experimentally identified in the beta decay of the Ga isotopes, are on the average about 0.5 MeV lower than the experimental values.

In fig. 3 the calculated results for the odd-mass Zn nuclei are shown. The experimental picture of ^{63}Zn is sketchy[28], most of the spin assignments being derived from beta-decay data. The available ℓ-values from the ^{64}Zn(p,d) [ref. [21,36]] and ^{64}Zn(^{3}He,α) experiments,[28,37] can not give more constraints because of inadequate energy resolution. Less dense spectra occur for ^{65}Zn and ^{67}Zn, where the low-lying levels are experimentally better known[30,32]. Here, the structure of the low-lying levels has been described[4,5] in terms of a weak-coupled $0f_{5/2}$, $1p_{3/2}$, or $1p_{1/2}$ neutron to an excited ^{64}Zn or ^{66}Zn core. However, the overall agreement with experiment is much better in the present calculation, where no parameters are adjusted to the specific properties of any of the Zn isotopes.

The occurrence of a low-lying $9/2^+$ state in both ^{65}Zn and ^{67}Zn gives a measure of the importance of the $0g_{9/2}$ orbit for this mass region. The spectra of ^{65}Zn and ^{67}Zn may also be compared with shell-model results[10-13] for ^{63}Ni and ^{65}Ni, respectively, since on the basis of the experimental spectra, the two protons outside the ^{56}Ni core apparently do not contribute significantly to the structure of the low-lying levels. The present calculation confirms this assumption since the contributions of the two protons to the total angular momentum of the ground state are only 8% and 6% for ^{65}Zn and ^{67}Zn, respectively.

To summarize, the overall agreement between experiment and calculation for ground and excited state energies of the A=62-68 Zn nuclei is surprisingly good, particularly in view of the fact that no Zn data have been used in the determination of the effective two-body matrix elements and single-particle energies.

In addition to calculations of energy levels of the A=62-68 isotopes which are experimentally well known, predictions are also made for ^{60}Zn and ^{61}Zn. As indicated in fig. 4, no excited states in ^{61}Zn are experimentally known[38]; the calculated value for the binding energy of the $J^{\pi}=3/2^{-}$ ground state, does agree with experiment. For ^{60}Zn, more experimental data are available[39]. Many levels below 5 MeV excitation energy are predicted by the present model. However, only a few levels have been experimentally observed in that region.

3. Single-Nucleon Spectroscopic Factors

The comparison of experimental and theoretical spectroscopic factors for single-nucleon transfer provides the most definitive test for model wave functions. In particular, the predicted relative occupations of the various shell-model orbits, the *sine qua non* of any microscopic calculation based on the shell-model idea, are thus tested. Spectroscopic factors provide in general information on whether the dominant components of the model wave functions are consistent with the observed properties of the corresponding experimental levels. Electromagnetic transition rates only provide information on integral properties of states and are not directly related to the specific orbits of the model wave functions. In the present paper no renormalization has been

applied to the calculated spectroscopic factors; simple creation operators have been used for each of the different shell-model orbits.

The experimental values for spectroscopic factors are obtained from analysis of measured differential cross sections of direct-reaction transfers of single nucleons in the frame of the distorted-wave Born approximation (DWBA) theory. For strong transitions, this determination involves errors of at least 20-30% in the derived values as a result of the uncertainties in the applied theory. For weak transitions even larger uncertainties may enter due to processes beyond the scope of DWBA, such as compound nucleus and pre-compound effects and coupled-channel and other multistep processes. In case of the Zn isotopes, the accuracy of the available data from neutron pick-up[20,21,36,37] is not as high as for the data from neutron stripping reactions[19,40,41]. For ^{64}Zn and ^{66}Zn, two sets of data on proton stripping[42,43] are also available, but the values of the ground-state transitions are not in agreement between the two references and also mutually disagree with the results of the proton pick-up reaction[44].

From experimental results on summed single-particle strengths in the different orbits observed in pick-up and stripping reactions, upper and lower limits on the particle occupation numbers of those orbits can be calculated. In the case of stripping reactions on a target with isospin T_o, the total strengths $G\rho^{+}(\pi,T_{<})$ for proton transfer and $G\rho^{+}(\nu,T_{>})$ for neutron transfer to orbit ρ, leading to final states with $T_{<}=T_o-1/2$ and $T_{>}=T_o+1/2$, respectively, obey the sum rule[45],

$$G\rho^{+}(\pi,T_{<}) + (2T_o+2)(2T_o+1)^{-1}G\rho^{+}(\nu,T_{>}) = \langle\rho\rangle^{-1}. \qquad (1)$$

The right hand side of this equation stands for the total number of proton and neutron holes in orbit ρ of the target state. However, the actual total strengths may not be experimentally observed, so that the actual number of holes can be larger than the value derived from this sum rule.

The total observed neutron stripping strength $G\bar{\rho}^{+}(\nu,T_{>})$ immediately provides a lower limit on the number of neutron holes in orbit ρ. Thus these two rules together provide, assuming the validity of the shell-model, upper limits on the occupation numbers of both neutrons and protons in orbit ρ of the target state.

From the observed pick-up from orbit ρ on the same target state, the total strengths $G\bar{\rho}(\pi,T_{>})$ and $G\bar{\rho}(\nu,T_{<})$ for proton and neutron transfer, respectively, provide lower limits on the occupation numbers in orbit ρ of the target state. Here, the value of $G\bar{\rho}(\pi,T_{>})$ immediately provides a lower limit on the number of protons in orbit ρ, while the right hand side of the equation (1) above yields a lower limit on the total number of protons and neutrons in orbit ρ if one replaces $G\bar{\rho}^{+}(\pi,T_{<})$ and $G\bar{\rho}^{+}(\nu,T_{>})$ by $G\bar{\rho}(\nu,T_{<})$ and $G\bar{\rho}(\pi,T_{>})$, respectively. In table 1 a comparison between the calculated ground-state occupation numbers and the upper and lower limits as derived from the experimental data with these sum rules is presented.

The lower limit on the total number of protons in the ground states of ^{64}Zn and ^{66}Zn is larger than two. This could result from the presence of proton holes in the $0f_{7/2}$ orbit and the consequent overflow into the higher fp orbits, consistent with the conclusions of the Hartree-Fock Bogoliubov (HFB) calculations of

refs. [6-9]. However, this "experimental" result depends upon the absolute normalization of the DWBA analysis used for the pick-up data[44] employed, and this is not a well determined factor. Also, stripping reactions[18,19] on the Zn isotopes give no evidence for either proton or neutron $f_{7/2}$ holes (a result independent of DWBA factors to first order) except for, perhaps, ^{68}Zn. There is, on the other hand, clear experimental evidence for the admixture of particles in the $0g_{9/2}$ orbit to the ground-state configurations of ^{66}Zn and ^{68}Zn.

As shown in table 1, experiment and our calculations agree in assigning the majority of the active protons to the $1p_{3/2}$ orbit. The calculated configuration mixing of the protons decreases slowly with increasing neutron number as can be seen in fig. 5: the average occupation of the proton $1p_{3/2}$ sub-shell is predicted to slowly increase with increasing mass of the Zn ground states. This decrease in configuration-mixing is also obtained in the calculations of refs. [8,9]. The agreement between the present calculated results and the experimental values on neutron occupation limits is better than for protons. However, the values in table 1 also show that the calculated neutron occupation numbers for the $1p_{3/2}$ and $1p_{1/2}$ orbits are somewhat larger than the corresponding "experimental" numbers. The largest deviation (35%) in these numbers is found for the ground state of ^{68}Zn which may be additional evidence for admixtures of $0g_{9/2}$ configurations in that state. The number of $0f_{5/2}$ neutrons in the ground states is reproduced particularly well. It can be seen in fig. 5 that the calculated neutron occupation numbers for the $1p_{1/2}$ and $0f_{5/2}$ orbits smoothly increase with increasing mass number.

In contrast, the occupation number of the $p_{3/2}$ neutron orbit increases more in the case where a neutron is added to an even mass isotope than when one is added to an odd-mass isotope.

We can go beyond a comparison of the total single-particle strengths to a comparison of predicted and observed strengths for individual levels. Comparison of relative strengths, beyond yielding information on individual states, has the advantage that many of the uncertainties of DWBA analysis are cancelled out. In tables 2 and 3 available data from pick-up and stripping reactions on Zn isotopes have been compared with results of the present calculations. For the odd-mass isotopes, as shown in table 2, only neutron pick-up and stripping data are known. In case of ^{63}Zn the available data have been obtained from experiments[21,28,36,37] with relatively poor resolution and large uncertainties in the applied DWBA analysis. The triplet at 0.64 MeV excitation energy (see fig. 3) was not resolved. However, the total observed ℓ=1 strength for those states is in good agreement with the summed strengths as calculated for the second $1/2^-$ and $3/2^-$ states. Also, the first excited $1/2^-$ state at 0.25 MeV has not been observed in the transfer experiment, but this may be because the very strong excited $5/2^-$ state is separated from it by only 55 keV.

More accurate data on both stripping and pick-up are available for ^{65}Zn. Here, as for ^{63}Zn, the $0f_{5/2}$ single-neutron strength is almost exhausted by the first $5/2^-$ state in both the experimental and model results. No ℓ=3 strength is observed for the first $7/2^-$ state. This is consistent with the assumption of a

closed ^{56}Ni core in the particle configurations of the low-lying states and, in particular, with an $f_{5/2}$-$p_{3/2}$-$p_{1/2}$ character for this $7/2^-$ state. It should be noted that the first two calculated $1/2^-$ states in ^{65}Zn appear, on the basis of their spectroscopic factors, to be inverted in energy relative to the first two experimental $1/2^-$ levels. Parenthetically, it is obvious that by omitting the oldest stripping data of ref. [40], as shown in table 2, the agreement between experiment and theory is improved.

For ^{67}Zn, as shown in table 2, the predicted pick-up strengths of the first $1/2^-$ and $3/2^-$ states are factors of 2 and 6 too strong, respectively, while the predicted values for the second and third $1/2^-$ and $3/2^-$ states agree with experiment. Since the quoted pick-up experiments[21,46] could easily separate the first $1/2^-$ and $3/2^-$ states from the strongly populated $5/2^-$ ground state, this deviation is a clear failure of the present model. A possible explanation is that the actual number of neutrons in the $1p_{1/2}$ and $1p_{3/2}$ orbits is smaller than calculated, due to two neutron excitation to the $0g_{9/2}$ orbit. Such a reduced occupation would be in agreement with the observed neutron-hole strengths for $1p_{1/2}$ and $1p_{3/2}$ orbits.

In table 3 a comparison is made between the calculated and experimental spectroscopic factors for transfer from odd-mass targets to states of the even-mass Zn isotopes. This comparison is not as unambiguous as for the odd-mass isotopes because of possible ℓ-mixtures in the observed single-particle transfer angular distributions and because of the lack of distinction between $1p_{1/2}$ and $1p_{3/2}$ transfers. None-the-less, here also the

spectroscopic factors provide quite a bit of insight into the validity of individual wave functions. As shown in table 3, the first two calculated eigenstates of each spin 0^+, 2^+ and 4^+ in ^{64}Zn can be securely identified with the experimental levels corresponding in energy by virtue of the correspondences in their associated spectroscopic factors. For higher excited states, the sequential matching of model eigenstates and experimental levels is not well defined, (as the case of the third 0^+ state illustrates).

For ^{66}Zn, both stripping and pick-up data are available. Here, the calculated fourth 0^+ and fifth 2^+ states have been identified with the experimental levels at 2.37 and 2.94, respectively. The level in ^{66}Zn at 2.77 MeV excitation energy has a strong ℓ=1 strength for pick-up and has been tentatively assigned as $(3^+,4^+)$ in ref. [26]. The calculated spectroscopic factors for pick-up leading to 3^+ states are very small, while the second model 4^+ state has a large $1p_{3/2}$ pick-up strength. Thus we may identify the level at 2.77 MeV with this second 4^+ state. The known 4^+ level at 3.08 MeV should consequently correspond to the third model 4^+ state. Here, also the calculated and observed spectroscopic strengths coincide. The observed low-lying states in ^{66}Zn in general appear to correlate well with the calculated spectrum on the basis of the spectroscopic factor comparison.

For ^{68}Zn only a few stripping data are known. The experimental strengths of the 2^+ states are stronger than predicted, indicating more 1p holes in the ground state of ^{67}Zn than calculated, as also can be seen from table 1. The failure to observe

strength for the 0^+ state at 1.66 MeV may be explained as due to strong $(1p_{3/2})^6$, $(0f_{5/2})^4$, $(0g_{9/2})^2$ admixtures in the particle configuration of that state.

In conclusion, one may say that the present model is, even without the possible $0f_{7/2}$ hole and expected $0g_{9/2}$ particle excitations, quite adequate in describing the energies and the major components of the wave functions of the low-lying states of the Zn isotopes with A=62-68. Only for the higher masses are the effects of the exclusion of the $0g_{9/2}$ orbit from the present configuration space evident.

4. Electromagnetic Properties

It was shown in the previous section that spectroscopic factors as well as energy levels for the A=62-68 Zn isotopes can be well reproduced in a model of active $p_{3/2}$, $p_{1/2}$, and $f_{5/2}$ orbits which uses the effective two-body matrix elements of ref. [16]. An appropriate issue to investigate after thus establishing that the model wave functions have certain key features consistent with nature is that of whether effective one-body operators exist with which the observed electromagnetic properties of these nuclei can be reproduced. Procedures for empirically determining effective values for various one-body operators have been discussed in detail in refs. [13] and [47]. The effective proton (e_p) and neutron (e_n) charges for E2 transitions and electric quadrupole moments and the effective reduced single-particle matrix elements for the M1 operator have been similarly obtained in the present paper from least-squares fits to available experimental data.

4.1. Electric Quadrupole Transitions and Moments

The number of E2 strengths and quadrupole moments experimentally known for the Zn isotopes is not large. Only 16 values have reasonably small uncertainties. These data include the B(E2) values of the ground-state transitions of the 2_1^+ and 2_2^+ states in ^{64}Zn, ^{66}Zn and ^{68}Zn, noted in tables 4b, 4c and 4d, respectively. From the odd-mass nuclei, in addition to the quadrupole moments of the ground states in ^{63}Zn, ^{65}Zn and ^{67}Zn, seven B(E2) values have been taken (see table 5). These are from the ground-state transitions of the $1/2_1^-$, $3/2_1^-$ and $3/2_2^-$ states in ^{65}Zn, the transition between the $3/2_1^-$ and the $1/2_1^-$ state in ^{67}Zn and from the ground-state transitions of the $3/2_1^-$, $5/2_2^-$ and $7/2_1^-$ states in the same nucleus. Because of the scarcity of E2 data, no attempt has been made to fit the E2 reduced single-particle matrix elements separately. However, a least-squares fit on one or both of the state independent effective charges is feasible. For the calculation of the isoscalar and isovector parts of the transition matrix elements for each isotope, reduced single-particle matrix elements of the E2 operator have been used which were calculated from harmonic-oscillator wave functions with $\hbar\omega=41A^{-1/3}$.

With the assumption that the effective charges satisfy the condition $e_p-e_n=1$, the values $e_p=1.8$ and $e_n=0.8$ were found, (all values given in units of the elementary charge), from making a one-parameter fit to the 16 pieces of E2 data. These values were also found from a calculation of the Cu isotopes[48] which used the same model as employed here. Actually, the available Zn data are sufficient to fix both effective charges and in so doing we find that the constraint $e_p-e_n=1$ is not optimal. This

is consistent with the result that the additional charge $\Delta e_n(\equiv e_n)$ of the neutron due to core polarization is larger than $\Delta e_p(\equiv e_p-1)$ calculated with perturbation theory[49]. When we treat e_p and e_n as independent parameters in a least-squares fit to the 16 pieces of E2 data, we obtain the values $e_p=1.6\pm0.2$ and $e_n=1.0\pm0.1$. The quoted uncertainties correspond to the values found at $\chi^2_{min}+1$, where χ^2_{min} is the minimum value of the chi-square deviation. We note that a relative error of 10% has been assigned to all the experimental transition matrix elements and moments used in the least-squares fit.

From these same E2 data treated in still another way a mass dependence of the effective neutron charge can be determined (fig. 6). The values for e_n have been obtained from a least-squares fit to the data in each isotope with a fixed value of $e_p=1.6$ for the proton charge. The error bars in fig. 6 correspond to the previously mentioned uncertainty of 0.2 in the value of e_p. This apparent reduction of the effective charge of the neutron as a function of increasing A (see fig. 6) might be explained as a decrease in the contribution of the ^{56}Ni core excitations. If the neutron effective charge is fixed as $e_n=1.0$ and the optimum proton effective charge is determined for each nucleus separately, only a negligible mass dependence of the effective proton charge is found. For ^{68}Zn a slightly larger value of $e_p=2.0\pm0.2$ gave the best agreement with experiment; this higher value may be explained by the increasing influence of $0g_{9/2}$ configurations for the higher masses. With the values of $e_p=1.6\pm0.2$ and $e_n=1.0\pm0.1$ as found from the A-independent least-

squares fit, values of B(E2) for transitions between states in ^{62}Zn, ^{64}Zn and ^{66}Zn have been calculated and tabulated in the tables 4a, 4b, and 4c, respectively. For ^{68}Zn, however, values have been calculated with the same neutron charge of 1.0 but with a value of 2.0±0.2 for the proton charge, as shown in table 4d.

The present calculation predicts strongly enhanced in-band B(E2) values, as is shown in the tables 4a, 4b, 4c and 4d. The average strength of the transitions between the second eigenstates of each J value decreases slowly with increasing mass number. This effect is presumably due to an exhaustion of the configuration space which occurs because the number of holes in the orbits of the present model space decreases with increasing mass number in this region. Evidence for this decrease in configuration mixing is also found in the enhancement with respect to the single-particle value of the B(E2; $2_1^+ \rightarrow 0_1^+$), which is 2.9 for ^{64}Zn but 1.9 for ^{68}Zn. (These values do not yet take into account the extra enhancement from the use of effective charges.) The failure of the present model in reproducing the value of the B(E2; $2_2^+ \rightarrow 0_2^+$) in ^{68}Zn, see table 4d, may be also due to the omission of excitations to the $0g_{9/2}$ orbit in the present configuration space.

The vibrational aspects of the even Zn isotopes are illustrated by the experimentally observed inhibition of the $2_2^+ \rightarrow 0_1^+$ cross-over transitions. This inhibition is also found in the present model results, since we obtain ratios B(E2; $2_1^+ \rightarrow 0_1^+$)/ B(E2; $2_2^+ \rightarrow 0_1^+$) of 100, 540 and 34, in comparison to the corresponding experimental ratios of 90, 360 and 31 for ^{64}Zn, ^{66}Zn and ^{68}Zn, respectively. However, the calculated values of the ratios

B(E2; $2_2^+ \rightarrow 2_1^+$)/B(E2;$2_2^+ \rightarrow 0_1^+$) are too small. We obtain ratios of 55, 520 and 44, in comparison to the experimental ratios of 160, 9200 and 31 for ^{64}Zn, ^{66}Zn and ^{68}Zn, respectively.

The large calculated value for B(E2; $0_2^+ \rightarrow 2_2^+$) found in ^{64}Zn (see table 4b) is explained by the large seniority $\nu = 4$ and 6 components in the wave function of the 0_2^+ state. This enhancement is not found for the 0_2^+ states in the other even-mass Zn isotopes since they contain mainly $\nu=0$ components. This sort of behaviour of 0_2^+ states was also reported from a calculation on Ni isotopes[13] with the same configuration space as the present one. There, the 0_2^+ in ^{62}Ni had similar properties to the one in ^{64}Zn.

In table 5 a comparison has been made between experimental and calculated B(E2) values for transitions in the odd-mass isotopes. Shown also are the results of a recent quasiparticle-phonon-coupling (QPC) calculation[5]. It should be noted that for ^{65}Zn the wave functions of the second and first $1/2^-$ states have been interchanged as suggested from the spectroscopic factors (see table 2). The overall agreement with experiment is fair when account is taken of the uncertainties in the experimentally deduced B(E2) values in ^{65}Zn due to large errors in the mixing ratios[30]. The more accurately determined B(E2) values are the ones from Coulomb excitation[5] and those transitions which are a purely E2. These values are much better reproduced by the present model than are those with larger experimental uncertainties. The general agreement of the values of the QPC calculation[5] with experiment is good. The QPC values were obtained from a model in which the relevant model parameters were adjusted to the properties of ^{67}Zn.

It should be mentioned that in case of ^{65}Zn the present calculations indicate that only neutrons contribute to the E2 transitions between the low-lying states. This is not the case for the other isotopes, where both protons and neutrons contribute to the transition.

The experimentally observed static electric quadrupole moments of the odd-mass ground states could only be reproduced with an effective charge for the neutron which was twice as large (e_n=2.1) as that found to fit the B(E2) values. The values of the quadrupole moments of low-lying states in the Zn isotopes have been calculated with e_p=1.1 and e_n=2.1 as well as with e_p=1.6±0.2 and e_n=1.0±0.1 and both sets of values are tabulated in table 6. Also quoted are the results of two recent Hartree-Fock Bogoliubov calculations[8,9] made in a full 0f-1p configuration space with different residual interactions. The values from the calculation of ref. [8], where projection of good angular momentum was employed, agree with the results of the present calculation, since both calculations predict, in terms of the rotational model, a prolate intrinsic shape for the even-mass Zn nuclei. This shape is confirmed in case of ^{64}Zn, where a negative value of the static quadrupole moment of the 2_1^+ state has been found[2]. Typical for the even-even nuclei are the opposite signs of the quadrupole moments of the first and second 2^+ states shown in table 6.

The decrease as a function of mass of the absolute values of the quadrupole moments of the 2^+ states in the even-mass Zn isotopes, a feature predicted by the HFB as well as by the present calculations, may be only a consequence of the exhaustion of the configuration space used and hence unphysical. An indication

that the quadrupole moments of these states remains large may be found from the value of -21±3 e fm^2 [ref. [2]], for the 2_1^+ state in ^{70}Zn, an absolute value larger than that of the 2_1^+ state in ^{64}Zn. However, for the quadrupole moments of the first $5/2^-$ states a clear mass dependence is found both experimentally and theoretically. This results from the change from a $f_{5/2}$-particle character to a $f_{5/2}$-hole character of the configuration of these states, when going from ^{63}Zn to ^{67}Zn.

4.2. Magnetic Dipole Transitions and Moments

Reliable data on M1 transition strengths in the Zn isotopes are not numerous (see table 5). Most of the data are lower limits or are deduced from experimentally known B(E2) values and mixing ratios with appreciably large errors. However, values of seven magnetic dipole moments (see table 6) are experimentally known[54,55]. Most of the model values for these cases turn out to be too large compared with experiment when calculated with an unrenormalized M1 operator. However, the calculated signs do agree with experiment, except for the magnetic moment of the $3/2_1^-$ state in ^{67}Zn. It should be recalled that the model wave function of this state also could not reproduce the value of its experimental spectroscopic factor (see table 2). With the unrenormalized M1 operator and the present model wave functions the correct sign is predicted for seven out of ten experimentally known mixing ratios, even when the predicted B(M1) values deviate strongly from experiment. This sign follows theoretically from the relative phases of the E2 and M1 transition matrix elements, where the convention of Rose and Brink[56] has been used in the present calculation. Again

observables related to the $3/2_1^-$ state in ^{67}Zn are badly reproduced with the present model wave functions since the calculated signs of the mixing ratios, in both transitions from this state, disagree with experiment (see table 5). The other disagreement in sign of the mixing ratio is found for the ground-state transition of the $3/2_2^-$ state in ^{67}Zn, however, the calculated B(M1) value is very small. For such small B(M1) values it should be remembered that the end result of the model calculation represents the incoherent sum of many largely canceling components. As such, the answer can be extremely sensitive to minor numerical details of the wave functions.

We have attempted to determine if an empirically renormalized, mass independent, M1 operator can yield better agreement with experiment than the bare-nucleon values when used with the present model wave functions.

We note that the M1 operator in the present case is, in contrast with similar calculations in the sd shell[47], affected by core polarizations through the first-order perturbation effect of the allowed $0f_{5/2} \rightarrow 0f_{7/2}$ single-particle M1 transition. There are not enough M1 data from the Zn isotopes to make an empirical determination of the ten single-particle matrix elements of the M1 operator via a least-squares fit feasible. It was found that empirical adjustment of the spin and orbital g-factors of protons and neutrons individually does not lead to improvement of the calculated values (see also ref. [13]). Since the matrix elements of the $0f_{5/2} \rightarrow 0f_{5/2}$ single-particle transition should be principally affected by excitations of the ^{56}Ni core, the isoscalar and isovector single-particle matrix elements for this orbit were ultimately

treated as free parameters in a least-squares fit to a data set comprised of the seven magnetic moments. The other eight matrix elements were simultaneously varied in the constraint of separate multiplicative adjustment factors for the isoscalar and isovector groups of matrix elements. From this four-parameter fit effective values of 1.48 and -1.94 were obtained for the reduced matrix elements of the $0f_{5/2} \rightarrow 0f_{5/2}$ M1 single-neutron and single-proton transition, respectively. The present renormalized value of the matrix element of the $0f_{5/2} \rightarrow 0f_{5/2}$ neutron transition, relative to the bare-nucleon value of 2.74, represents a slightly smaller quenching than that obtained[13] for the Ni isotopes, where a value of 1.03 was found.

The adjustment factors for the isoscalar and isovector groups of the remaining matrix elements of the M1 operator are 1.47 and 0.84, respectively. The largest change of a matrix element which results from these adjustments is in the $1p_{3/2} \rightarrow 1p_{3/2}$ single-neutron transition, which is quenched to a value of -1.81 from the bare-nucleon value of -3.41; this may be compared with the value of -1.61 found in ref. [13]. It should be noted that the vanishing of the ℓ-forbidden M1 matrix element for the $1p_{3/2} \rightarrow 0f_{5/2}$ transition is not affected by the present fitting procedure. A non-zero value of this matrix element would affect the calculated results, since the contribution of this transition to the total M1 strength is quite large and in many cases comparable to one from $0f_{5/2} \rightarrow 0f_{5/2}$ transition. The present calculations indicate that M1 transitions between states with $J^\pi = 3/2^-$ and $5/2^-$ will be particularly affected if a non-zero matrix element for the $1p_{3/2} \rightarrow 0f_{5/2}$ transition is allowed. However, no consistent value for this matrix element could be

extracted from the few available data on M1 transition strengths. It is possible that a least-squares fit to all experimentally determinable M1 transition strengths and dipole moments in the Ni, Cu and Zn isotopes would lead to a fixed determination of all the ten M1 effective reduced single-particle matrix elements.

With the effective M1 matrix elements determined from the four-parameter fit, better agreement is obtained between model results and experimental values for the magnetic dipole moments, as is shown in table 6. However, in case of the dipole moments of the two $3/2^-$ states in ^{65}Zn, the altered matrix elements yield moments which are too large. The predicted values for the dipole moments of the first-excited 2^+ states in the even-mass Zn isotopes contain only a small isovector contribution. This results from the almost equal values of the projections of the total angular momenta of the proton and the neutron configurations along the quantization axis, both being about one in the present cases, and the fact that the isovector part of the dipole moment can be written as a term proportional to the difference of these two projections. The values of the isoscalar part, μ_o, of the dipole moments of those 2^+ states are within the limits $\mu_o = +1.00 \pm 0.16\ \mu_N$ found in other calculations[57] on 2^+ states in even-even nuclei. Lifetimes of about 2 ps and the decay to a $J^\pi = 0^+$ ground state make these 2^+ states promising candidates for experimental determination of their g-factors by means of an ion-implantation perturbed angular correlation technique[58].

The improvement obtained in the calculated M1 transition strengths by using the present effective M1 operator is not significant. In particular, the very small values ($5 \times 10^{-3}\ \mu_N^2$, see table 5), did not change significantly.

It is apparent from the results shown in table 5, that a definitive comparison between experiment and the present model results for M1 transitions is hampered by the lack of adequate experimental data. Larger M1 strengths than those observed until now would be more suitable for comparison, since larger calculated M1 strengths are less sensitive to the "noise" in the wave functions.

5. Allowed Beta Decay

We discuss in this section the calculated log ft values for the allowed beta decays from the Ga to the Zn isotopes and their relationship to experimental values. Results are shown in table 7. Since only pure Gamow-Teller transitions are taken into account for this comparison, log ft values are calculated from the numerical relation, $\log ft = 3.62 - \log \langle\sigma\rangle^2$, where $\langle\sigma\rangle$ stands for the Gamow-Teller matrix element. The value 3.62 stems from the different constants in the theoretical expression for the ft value. The log ft values calculated from this relation with the present model wave functions and an unrenormalized Gamow-Teller operator are in qualitative agreement with experiment, except for the transitions between $J^\pi = 3/2^-$ and $5/2^-$ states. However, for this kind of transition, the single-particle transitions $0f_{5/2} \rightarrow 0f_{5/2}$ and $1p_{3/2} \rightarrow 0f_{5/2}$ are found from the calculated transition matrix element to be very important. Hence, these decays are significantly affected by excitations of the ^{56}Ni core in a similar fashion to that discussed for the M1 transitions. However, unlike the M1 case, a search for empirical effective Gamow-Teller single-particle matrix elements yielded no improve-

ment in agreement between experiment and theory for these beta decays.

The choice of another value for the ratio of the axial-to vector-coupling constants will not improve agreement with experiment in the present case, since this would only add a constant factor to all the calculated log ft values. It should be noticed that the log ft values for the Gamow-Teller transitions to the 1^+ states are the only experimental observables, excluding the excitation energies, which are available for these states. The agreement obtained between model and experiment is good so far as one accepts the spin assignments in table 7. Finally, we note that the transitions to the $3/2^-$ states in ^{67}Zn are not badly reproduced by the model, in contrast with the case for the M1 transitions from these states (see sect. 4.2.).

It is not clear what conclusions can ultimately be drawn from comparisons of calculated and observed beta-decay rates in this region and in the present model context. Even the strongest transitions (log ft ≈5) are rather weak in terms of a pure single-particle value ($p_{3/2}\rightarrow p_{1/2}$; log ft=3.4). The well established need for significant renormalization of the σ operator together with the congenital sensitivity of the total matrix element, $\langle\sigma\rangle$, to minor details in the wave function amplitudes may combine to inhibit the obtaining of information about either the operator or the wave functions via this route.

6. Summary and Conclusions

An effective empirical interaction determined from the spectra of the Ni and Cu isotopes has been applied in the full $1p_{3/2}$-$0f_{5/2}$-$1p_{1/2}$ model space to the problem of calculating the binding energies and wave functions of the low-lying levels in the A=62-68 Zn isotopes. The average absolute deviation between the calculated and experimental ground-state binding energies is 0.19 MeV and the calculated excitation energies are generally in good agreement with the experimental spectra. Hence, as far as energies are concerned, the effective Hamiltonian based on levels in the Ni and Cu isotopes accounts in equivalent fashion for features of neighbouring nuclei. The ground-state binding energies obtained in this calculation agree better with experimental values than do the results of Hartree-Fock Bogoliubov calculations in a full 1p-0f model space. The worst differences (≈0.5 MeV) between experimental and calculated excitation energies are found for some of the second 0^+ and third 2^+ states in the even-mass nuclei. These problems can possibly be explained as consequences of the omission of $(0g_{9/2})^2_{0,1}$ and $(0g_{9/2})^2_{2,1}$ admixtures, respectively, from the model space.

The consistency of the dominant components of the present model wave functions with the experimentally observed properties of the corresponding state is demonstrated by the agreement, within experimental uncertainties, between most calculated and experimental values of spectroscopic factors of single-nucleon transfer. Both the total ground-state occupation distributions over the fp orbits and the detailed distribution of single-particle and single-hole strengths in the residual spectra are generally well reproduced. The deviations which appear most substantive occur for the heavier isotopes where, consistent with the evidence from

the energy level spectra, it can be expected that $0g_{9/2}$ admixtures begin to play a more significant role in the structure of the various levels.

The extent of validity of the $1p_{3/2}$-$0f_{5/2}$-$1p_{1/2}$ space for the Zn isotopes was further examined by comparing matrix elements of the E2, M1 and Gamow-Teller operators, calculated with the model wave functions, with corresponding experimental values. As expected, use of the bare values of the E2, M1 and the Gamow-Teller operators did not lead to close agreement between model and experimental results. The use of effective E2 charges of $e_p=(1.6\pm0.2)e$ and $e_n=(1.0\pm0.1)e$ yields calculated quadrupole moments and B(E2) values which agree reasonably well with a range of such data which encompasses both large and small expectation values. Certain vibrational features of these nuclei emerge of these E2 calculations. The most obvious discrepancies between model and experimental results involve the quadrupole moments of the odd-mass isotopes, which seem to call for a larger $e_n(\simeq 2.1\ e)$, and, again, the data for the heaviest isotopes. The present value for the E2 isoscalar charge of $e_p+e_n=2.6$ was also found from a calculation[48] on the Cu isotopes which used the same model space as employed here. However, a larger value of $e_n=1.7$, as compared with the present one ($e_n=1.0$), was found from a similar calculation[13] on the Ni isotopes.

There are considerably fewer useful experimental data on M1 and Gamow-Teller matrix elements for the Zn isotopes. A rather crude alteration of the M1 single-particle matrix elements brought about improved agreement between calculated and measured magnetic

moments, but the few, quite weak, observed M1 transitions remained poorly predicted. The observed G-T log ft values are on the whole matched, in a strong-weak sense, by the model results. Here, however, no determinable alteration of the single-particle matrix elements improved the picture. It remains to be determined in the light of more extensive data whether effective M1 and G-T operators will, together with the present model, suffice to give an overall accounting for these phenomena.

It is clear from the present work that many of the most obvious features of the Zn isotopes are well explained in terms of a $1p_{3/2}$-$0f_{5/2}$-$1p_{1/2}$ shell model and that parameters of such a model determined purely from Ni and Cu data extend to Zn with remarkable accuracy. This demonstration of the potential for extrapolation of the shell-model scheme is perhaps the most significant result of the present work. There are, concurrent with this successful reproduction of the average features of the Zn isotopes, clear instances of deficiencies of the present calculation.

To an extent, these deficiencies clearly involve the model space limitations. The omission of the $0g_{9/2}$ orbit should be a significant problem on general grounds and the poorer agreement between model and experiment for the heavier isotopes is consistent with such an expectation. There is no explicit evidence on $0f_{7/2}$ (^{56}Ni core) excitations in the low-lying Zn levels. The previous[16] work on Ni and Cu, together with our results for the lighter Zn isotopes seem to be consistent with the assumption that first order admixtures are not large. The $0f_{7/2}$ orbit can none-the-less have important effects on the present calculations through its

action in renormalization of the Hamiltonian and the various one-body operators.

Finally, in consideration of the deficiencies of the present calculations, it must be realized that the use of the exact Ni-Cu Hamiltonian for Zn does not allow the model space assumptions to be tested in the optimum fashion for the systems under present consideration. It seems clear in retrospect that a simultaneous fit to Ni, Cu and Zn levels would yield an altered Hamiltonian which would better reproduce, for example, the $1/2^-$-$3/2^-$-$5/2^-$ spin orderings of the ^{63}Zn low-lying levels, improve the excited 0^+ state spectra, etc. The extent to which such alterations would have corollaries in the wave functions and corresponding transition rates and moments remains to be determined.

REFERENCES

1. L.S. Kisslinger and K. Kumar, Phys. Rev. Lett. 19(1967)1239
2. J.W. Lightbody, Jr., Phys. Lett. 38B(1972)475
3. V.K. Thankappan and W.W. True, Phys. Rev. 137(1965)B793
4. A. Weidinger, E. Finckh, U. Jahnke and B. Schreiber, Nucl. Phys. A149(1970)241
5. M.J. Throop, Y.T. Cheng and D.K. McDaniels, Nucl. Phys. A239(1975)333
6. H. Chandra and M.L. Rustgi, Phys. Rev. C4(1971)874
7. H. Chandra and M.L. Rustgi, Phys. Rev. C6(1972)1281
8. J.K. Parikh, Phys. Rev. C6(1972)2177
9. T.S. Sandhu and M.L. Rustgi, Phys. Rev. C12(1975)666
10. N. Auerbach, Phys. Rev. 163(1967)1203
11. R.D. Lawson, M.H. Macfarlane and T.T.S. Kuo, Phys. Lett 22(1966)168
12. S. Cohen, R.D. Lawson, M.H. Macfarlane, S.P. Pandya and M. Soga, Phys. Rev. 160(1967)903
13. P.W.M. Glaudemans, M.J.A. deVoigt and E.F.M. Steffens, Nucl. Phys. A198(1972)609
14. E.A. Phillips and A.D. Jackson, Phys. Rev. 169(1968)917
15. S.S.M. Wong, Nucl. Phys. A159(1970)235
16. J.E. Koops and P.W.M. Glaudemans, to be published and preliminary report 1973, Utrecht University
17. W. Chung and B.H. Wildenthal, unpublished, Michigan State University
18. R.G. Couch, et al., Phys. Rev. C2(1970)149
19. D. von Ehrenstein and J.P. Schiffer, Phys. Rev. 164 (1967)1374

20. M.G. Betigeri, et al., Nucl. Phys. A171(1971)401
21. J.C. McIntyre, Phys. Rev. 152(1966)1013
22. R.P. Singh, R. Raj, M.L. Rustgi and H.W. Kung, Phys. Rev. C2(1970)1715
23. M.L. Rustgi, et al., Phys. Rev. C4(1971)854
24. P.W.M. Glaudemans, P.J. Brussaard and B.H. Wildenthal, Nucl. Phys. A102(1967)593
25. Nuclear Level Schemes A=45 through A=247 from Nuclear Data Sheets, Edited by Nuclear Data Group, Academic Press, 1973
26. J.F. Bruandet, et al., Phys. Rev. C12(1975)1739
27. R.A. Hinrichs and D.M. Patterson, Phys. Rev. C10(1974)1381
28. R.L. Auble, Nucl. Data Sheets 14(1975)119
29. M. Agard, et al., Rapport Annuel 1974, ISN Grenoble (1975) p.55
30. R.L. Auble, Nucl. Data Sheets 16(1975)351
31. R.L. Auble, Nucl. Data Sheets 16(1975)417
32. R.L. Auble, Nucl. Data Sheets 16(1975)155
33. M.B. Lewis, Nucl. Data Sheets 14(1975)155
34. A.H. Wapstra and N.B. Gove, Nuclear Data Tables 9(1971)267
35. W.J. Courtney and J.D. Fox, Atomic Data and Nuclear Data Tables 15(1975)141
36. R.R. Johnson and G.D. Jones, Nucl. Phys. A122(1968)657
37. M.G. Betigeri, et al., Nucl. Phys. A100(1967)416
38. R.L. Auble, Nucl. Data Sheets 16(1975)1
39. H.J. Kim, Nucl. Data Sheets 16(1975)317
40. E.K. Lin and B.L. Cohen, Phys. Rev. 132(1963)2632

41. K.A. Gridnev, et al., Yad. Fiz. 8(1968)1101 in Soviet J. of Nucl. Phys. 8(1969)639
42. J.L.C. Ford, Jr., K.L. Warsh, R.L. Robinson and C.D. Moak, Nucl. Phys. A103(1967)525
43. V.V. Okorokov, et al., Yad. Fiz. 8(1968)869 in Soviet J. of Nucl. Phys. 8(1969)505
44. D. Bachner, et al., Nucl. Phys. A99(1967)487
45. M.H. Macfarlane and J.B. French, Revs. Mod. Phys. 32(1960) 567 and J.P. Schiffer in Isospin in Nuclear Physics ed. D.H. Wilkinson (North-Holland, Amsterdam 1969) p. 666
46. M. Borsaru, et al., Nucl. Phys. A237(1975)93
47. P.W.M. Glaudemans, P.M. Endt and A.E.L. Dieperink, Ann. of Phys. 63(1971)134
48. P.J. Brussaard, Proc. Int. Conf. on Nuclear Structure and Spectroscopy, vol. 2 (Scholar's Press, Amsterdam 1974) p. 489
49. K.W. Schmid and G. Do Dang, Z. Physik 268(1974)65
50. R. Neuhausen, Habilitationsschrift, Institut für Kernphysik, Universität Mainz, KPH 22/74 (August 1974)
51. A.K. Sen Gupta and D.M. Van Patter, Nucl. Phys. 50(1964)17
52. M. Ivascu, et al., Nucl. Phys. A218(1974)104
53. S. Roodbergen, et al., Z. Physik 275(1975)45
54. S.A. Wender and J.A. Cameron, Nucl. Phys. A241(1975)332
55. G.H. Fuller and V.W. Cohen, Nuclear Data Tables A5(1969) 433
56. H.J. Rose and D.M. Brink, Revs. Mod. Phys. 39(1967)306
57. J.F.A. van Hienen and P.W.M. Glaudemans, Phys. Lett. 42B (1972)301

58. G.K. Hubler, H.W. Kugel and D.W. Murnick, Phys. Rev. C9 (1974)1954 and J.L. Eberhardt, G. van MiddelKoop, R.E. Horstman and H.A. Doubt, Phys. Lett. 56B(1975)329

59. G.H. Dulfer, et al., Nucl. Phys. A182(1972)433

60. D. Basu, Nucl. Phys. A188(1972)97

FIGURE CAPTIONS

Fig. 1.--Binding energy differences of ground states given as $\Delta E_b(A)=E_b(A)-E_b(A-1)$. The experimental and theoretical differences are shown for the present calculations (ASDI) and for the Hartree-Fock Bogoliubov calculations (HFB) of ref. [9]. The differences for A=61 are given, both for theoretical and experimental energies, with respect to the experimental ground-state binding energy of ^{60}Zn. All the values used, are corrected for Coulomb energies.

Fig. 2.--A comparison between the calculated (ASDI) and the experimental excitation energies of the even-mass Zn isotopes. The experimental values have been taken from refs. [25-27,29,31,33] The calculated binding energy with respect to the ^{56}Ni core (given in brackets) corresponds to the lowest state with the J^{π} value of the experimental ground state. The binding energy of that state. also given, is corrected for Coulomb energies. Only calculated and experimental excitation energies less than 3.2 MeV are shown.

Fig. 3.--A comparison between the calculated (ASDI) and experimental excitation energies of the odd-mass Zn isotopes. The experimental values have been taken from refs. [28,30,32]. The quoted spin values are twice their physical values. For binding energies see the caption of fig. 2. Only calculated and experimental excitation energies less than 2 MeV are shown.

Fig. 4.--A comparison between the calculated (ASDI) and experimental excitation energies in ^{60}Zn and the predicted level scheme for ^{61}Zn. Only calculated and experimental excitation energies[39] less than 5 MeV are shown for ^{60}Zn. The quoted spin values are twice their physical values in case of the ^{61}Zn level scheme, where only excitation energies less than 2 MeV are shown. For the comparison of the binding energies see the caption of fig. 2.

Fig. 5.--Calculated occupation numbers for the protons and neutrons in the ground states of the Zn isotopes. In the present model only the $1p_{3/2}$, $0f_{5/2}$ and $1p_{1/2}$ orbit are active.

Fig. 6.--Mass dependence of the effective neutron charge (e_n) with a fixed value of the effective proton charge (e_p). Also those values for e_n are marked which gave a minimum value of the χ^2 in the least-squares fit to data from each of the Zn isotopes, when the value of e_p is not fixed.

TABLE 1

A comparison of calculated and observed occupation numbers in the ground states of some Zn nuclei

Nucleus	Subshell	Protons			Neutrons		
		Experiment[a]		ASDI	Experiment[a]		ASDI
		Lower limit	Upper limit		Lower limit	Upper limit	
^{64}Zn	$1p_{1/2}$	0.46 ± 0.11[b]		0.31	1.0 ± 0.2[e]		0.1
	$1p_{3/2}$	1.6 ± 0.4	2.6 ± 0.6[c]	1.28	1.8 ± 0.4	3.2 ± 0.8[f]	2.5
	$0f_{5/2}$	1.1 ± 0.3	0.5 ± 0.1[d]	0.41	3.0 ± 0.7	2.9 ± 0.7[g]	2.6
	$0g_{9/2}$	0.34 ± 0.09	4.1 ± 1.0	-		2.2 ± 0.6	-
^{66}Zn	$1p_{1/2}$	0.45 ± 0.11		0.26	1.3 ± 0.3		1.1
	$1p_{3/2}$	2.0 ± 0.5	2.2 ± 0.5[h]	1.36	2.7 ± 0.7	3.7 ± 0.9[f]	3.1
	$0f_{5/2}$	1.1 ± 0.3	0.10 ± 0.02[i]	0.38	4.3 ± 1.1	4.2 ± 1.1[g]	3.6
	$0g_{9/2}$	0.35 ± 0.09	4.4 ± 1.1	-	0.6 ± 0.2[j]	1.6 ± 0.4	-
^{67}Zn	$1p_{1/2}$			0.24		0.8 ± 0.2[k]	1.3
	$1p_{3/2}$			1.40	3.1 ± 0.8[l]	2.8 ± 0.7	3.5
	$0f_{5/2}$			0.36	0.9 ± 0.2	4.8 ± 1.2	4.0
^{68}Zn	$1p_{1/2}$		2.4 ± 0.6[c]	0.21	0.7 ± 0.2	4.8 ± 1.2[f]	1.5
	$1p_{3/2}$			1.43	2.3 ± 0.6		3.6
	$0f_{5/2}$		0.35 ± 0.09[d]	0.36	5.1 ± 1.3	4.8 ± 1.2[g]	4.7
	$0g_{9/2}$		4.1 ± 1.1	-	0.9 ± 0.2	1.0 ± 0.2	-

a) An internal error of 25% has been assumed for all the experimental data used. No separate upper limits could be given for the $1p_{1/2}$ and $1p_{3/2}$ orbit, since only the total $\ell=1$ strengths was obtained in the stripping experiments. For derivation of the upper and lower limits see text. Footnotes b), c), etc., apply to the entire column of entries under the footnoted entry up to the next footnote.

b) From (t,α) of ref. [44]. In case of ^{64}Zn the data have been multiplied with 0.8.

c) From (d,p) of ref. [41] and (d,n) of ref. [18].

d) From (d,p) of ref. [19] and (d,n) of ref. [18].

e) From (p,d) of ref. [21] and (t,α) of ref. [44]. The latter data are multiplied with a factor 0.8 in case of ^{64}Zn.

f) From (d,p) of ref. [41].

g) From (d,p) of ref. [19]

h) From (d,n) and (^{3}He,d) of ref. [18] and ref. [20], respectively and (d,p) of ref. [41].

i) The pick-up data from the previous entry but combined with (d,p) of ref. [19].

j) From ref. [20]

k) From ref. [40] but the uncertainty is larger than quoted, see text.

l) From (p,d) of ref. [21] and assuming two protons in the 1 $p_{3/2}$ orbit only.

TABLE 2

A comparison of experimental and calculated values of excitation energies and spectroscopic factors for single-neutron stripping (S^+) and pick-up (S^-) transfers to negative-parity states in odd mass Zn isotopes.

Nucleus	$J^\pi;T$	E_x (MeV)		$100\times S^+$		$100\times S^-$	
		ASDI[a]	Expt.[b]	ASDI	Expt.[c]	ASDI	Expt.[c]
^{63}Zn	$1/2^-;3/2$	0.34	0.25			33	
		0.94	(0.64)			24	59[d], 84[e], 80[f], 92[g]
		1.67				2	
	$3/2^-;3/2$	0	0			122	144, 135, 122, 126
		0.39	(0.63)			59	59, 84, 80, 92
		0.95	(1.03)			22	13, , 17,
	$5/2^-;3/2$	0.24	0.19			232	227, 280, 290, 312
		0.61	(0.65)			1	
		1.29				1	
^{65}Zn	$1/2^-;5/2$	0.73	0.05	15	34[h], 36[i]	17	37[e], 31[j]
		0.09	0.867	44	28 , 36	75	60, 60, 50[g]
		1.39		0		4	
	$3/2^-;5/2$	-0.08	0.12	29	17 , 34	204	220, 196, 194
		0.25	0.21	3	17 , 2	20	20, 26,
		0.90	0.91	3	, 5	38	, 12,
	$5/2^-;5/2$	0	0	52	21 , 52	326	410, 400, 391
		0.55	0.77	1		7	, 14, 35
		1.00	1.05	0.1		0.2	
^{67}Zn	$1/2^-;7/2$	-0.04	0.09	35	55[i]	112	40[e], 58[k]
		0.86	1.14	7	19	22	18 , 19
		1.40	(1.54)	0	2	6	, 3
	$3/2^-;7/2$	0.15	0.18	8	2	116	19 , 20
		0.41	0.39	11	26	181	176, 190
		1.11	(0.87)	0.4		3	4, 3
	$5/2^-;7/2$	0	0	39	30	426	380, 387
		0.80	0.89	0		0.5	
		1.21		0		3	

a) Energies are given with respect to the experimental ground-state binding energy.

b) Energies enclosed in parentheses indicate the lack of a firm experimental spin- parity assignment. The values are taken from the compilations of refs. [28, 30, 32].

c) Assignments of the ℓ-values are according to ℓ=1 for $1/2^-$ and $3/2^-$ states and ℓ=3 for $5/2^-$ states. Footnotes d), e), etc., apply to the column of entries till the data from the next nucleus.

d) From ref. [36]. The second $3/2^-$ and $1/2^-$ in ^{63}Zn could not be resolved in the pick-up experiments and so the same strength is noted twice.

e) From ref. 21)

f) From ref. 37), but with a normalization factor N=38.8.

g) From D.D. Borlin - Thesis, Washington University (1967). Values from the (^{3}He,α) reaction on ^{64}Zn and ^{66}Zn, as quoted in ref. 28) and ref. [20], respectively.

h) From ref. [40].

i) From ref. [19].

j) From ref. [20].

k) From ref. [46].

TABLE 3

A comparison of experimental and calculated values of excitation energies and spectroscopic factors for single-nucleon stripping (S^+) and pick-up (S^-) transfers to positive-parity states in the even - mass Zn isotopes.

Nucleus	J^π	E_x (MeV) ASDI[a]	E_x (MeV) Expt.[b]	Target	(100×S^+) / (100×S^-) ASDI $P_{1/2}$	ASDI $P_{3/2}$	ASDI $f_{5/2}$	Experiment[c] ℓ=1	Experiment[c] ℓ=3
^{64}Zn	0^+	0	0	^{63}Cu		152		172[d], 264[e]	
		1.72	1.91			1		10,	
		3.14[i]	2.61			56		34,	
	2^+	0.94	0.99		26	54	3	80, 111	
		1.84	1.80		6	0	0	17,	
		2.09	2.79		6	13	4	38*	
	4^+	2.21	2.31				32		47[d]
		2.49	2.74				1		0*
		2.85	3.08				52		239*
^{66}Zn	0^+	0	0	^{65}Cu/^{67}Zn	155/		/39	209[d], 119[e]/	/44[f], 27[g]
		3.15[i]	2.37			51/	/ 0	40, /	/ ,
	2^+	1.02	1.04		23/12	64/1	3/20	97, 49/10[f], 10[g]/	,
		1.70	1.87		12/5	4/0	0/3	29, 28/1, 1	/ ,
		2.87[j]	2.94		15/1	53/2	8/30	62, 83/ ,	/47, 22
	4^+	2.37	2.45			/17	29/6	/2, 2	40[d]/
		2.54	(2.77)			/57	3/39	/52, 55	
		2.76	3.08			/6	56/3	/10, 6	90 /
^{68}Zn	0^+	0	0	^{67}Zn			426		384[h]
		2.89	1.66				22		
	2^+	1.13	1.08		2	0	2	19[h]	
		1.60	1.88		16	1	10	14	
		2.74	2.34		2	0	19	17	
	4^+	2.49	(2.42)			4	20		
		2.67	(2.96)			0	6		

a) Energies are given with respect to the experimental ground-state binding energy.
b) Energies enclosed in parentheses indicate the lack of a firm experimental spin-parity assignment. The excitation energies have been taken from refs. [29, 31, 33].
c) Footnotes apply to the whole column of entries for the data in one nucleus. Values marked with an asterisk are the total strengths of multiplets not resolved by the experiment.
d) From ref. [42].
e) From ref. [43].
f) From ref. 21).
g) From ref. [46].
h) From ref. [40] but normalized w.r.t. the ground-state strength as found from the reverse reaction [21, 46].
i) In this case the fourth eigenvector has been used.
j) In this case the fifth eigenvector has been used.

TABLE 4a

Values of B(E2) for transitions between states in ^{62}Zn

E_{xi} → E_{xf} [a] (MeV)	J_i^π → J_f^π [b]	B(E2) with ADSI [c] (e^2fm^4)
0.95 → 0	$2_1^+ \to 0_1^+$	280 ± 50
1.80 → 0	$2_2^+ \to 0_1^+$	2.8 ± 1.2
→ 0.95	$\to 2_1^+$	70 ± 11
2.33 → 0.95	$0_2^+ \to 2_1^+$	57 ± 9
→ 1.80	$\to 2_2^+$	14 ± 2
2.81 → 0.95	$2_3^+ \to 2_1^+$	0.02 ± 0.12
→ 1.80	$\to 2_2^+$	2.9 ± 1.2
2.19 → 0.95	$4_1^+ \to 2_1^+$	370 ± 60
→ 1.80	$\to 2_2^+$	0.08 ± 0.02
2.74 → 0.95	$4_2^+ \to 2_1^+$	≈0
→ 1.80	$\to 2_2^+$	109 ± 17
(3.38) → 2.19	$6_1^+ \to 4_1^+$	310 ± 50
→ 2.74	$\to 4_2^+$	1.4 ± 0.4
3.97* → 2.19	$6_2^+ \to 4_1^+$	0.09 ± 0.07
→ 2.74	$\to 4_2^+$	190 ± 30

a) Excitation energies are taken from refs. [27, 29]. Values enclosed in parentheses indicate the lack of a firm experimental spin-parity assignment. Asterisks indicate values calculated with ASDI.

b) Lower indices denote the eigenvector number used in the calculation of the B(E2) value.

c) Calculated with harmonic-oscillator radial wave functions with $\hbar\omega = 41\ A^{-1/3}$ and effective charges of 1.6±0.2 and 1.0±0.1 for the proton and neutron, respectively. The single-particle estimate corresponds to a B(E2) value of 14 e^2fm^4.

TABLE 4b

Values of B(E2) for transitions between states in ^{64}Zn

E_{xi} → E_{xf} [a] (MeV)	J_i^π → J_f^π [b]	B(E2) (e^2fm^4) Expt.	B(E2) (e^2fm^4) ASDI [c]
0.99 → 0	$2_1^+ \to 0_1^+$	316 ± 10 [d]	290 ± 50
1.80 → 0	$2_2^+ \to 0_1^+$	3.5 ± 0.2 [d]	2.9 ± 1.7
→ 0.99	$\to 2_1^+$	560 ± 50 [e]	160 ± 20
1.91 → 0.99	$0_2^+ \to 2_1^+$		59 ± 9
→ 1.80	$\to 2_2^+$		510 ± 80
2.79 → 0.99	$2_3^+ \to 2_1^+$		0.8 ± 0.8
→ 1.80	$\to 2_2^+$		≈0
2.31 → 0.99	$4_1^+ \to 2_1^+$		390 ± 60
→ 1.80	$\to 2_2^+$		4.6 ± 0.7
2.74 → 0.99	$4_2^+ \to 2_1^+$		0.14 ± 0.02
→ 1.80	$\to 2_2^+$		38 ± 6
4.00 → 2.31	$6_1^+ \to 4_1^+$		360 ± 60
→ 2.74	$\to 4_2^+$		18 ± 3
3.87* → 2.31	$6_2^+ \to 4_1^+$		12 ± 2
→ 2.74	$\to 4_2^+$		103 ± 19

a) Excitation energies are taken from refs. [27,29]. The conventions of the presentation are explained under footnote a) in table 4a.

b) See caption of table 4a.

c) Similar to the calculations in table 4a. The single-particle estimate corresponds to a B(E2) value of 15 e^2fm^4.

d) From (e,e') experiment of ref. [50].

e) From the ratio $B(E2; 2_2^+ \to 2_1^+)/B(E2; 2_2^+ \to 0_1^+) = 159 \pm 12$ as reported in ref. [51] and the value of $B(E2; 2_2^+ \to 0_1^+)$ from ref. [50].

TABLE 4c

Values of B(E2) for transitions between states in ^{66}Zn

E_{xi} (MeV)	→	E_{xf} [a]	J_i^π	→	J_f^π [b]	B(E2) (e^2fm^4) Expt.	B(E2) (e^2fm^4) ASDI [c]
1.04	→	0	2_1^+	→	0_1^+	274 ± 10 [d]	270 ± 40
1.87	→	0	2_2^+	→	0_1^+	0.76 ± 0.12 [d]	0.5 ± 1.0
	→	1.04		→	2_1^+	≈7 x 10^3 [e]	260 ± 40
2.84*	→	1.04	0_2^+	→	2_1^+		71 ± 12
	→	1.87		→	2_2^+		38 ± 6
(2.70)	→	1.04	2_3^+	→	2_1^+		11 ± 3
	→	1.87		→	2_2^+		21 ± 3
2.45	→	1.04	4_1^+	→	2_1^+		330 ± 50
	→	1.87		→	2_2^+		0.05 ± 0.04
(2.77)	→	1.04	4_2^+	→	2_1^+		13 ± 2
	→	1.87		→	2_2^+		16 ± 3
4.18	→	2.45	6_1^+	→	4_1^+		320 ± 50
	→	(2.77)		→	4_2^+		0.2 ± 0.2
4.08*	→	2.45	6_2^+	→	4_1^+		10 ± 2
	→	(2.77)		→	4_2^+		65 ± 13

a) Excitation energies are taken from refs. [26, 31]. The conventions of the presentation are explained under footnote a) in table 4a.

b) See caption of table 4a.

c) Similar to the calculations in table 4a. The single-particle estimate corresponds to a B(E2) value of 16 e^2fm^4.

d) From (e,e') experiment of ref. [50].

e) From a mean life of τ_m=270± 100 fs [ref. [52]] and a 100% branch to the 1.04 MeV level with δ=+3 as quoted in ref. [31].

TABLE 4d

Values of B(E2) for transitions between states in ^{68}Zn

E_{xi} (MeV)	→	E_{xf} [a]	J_i^π	→	J_f^π [b]	B(E2) (e^2fm^4) Expt.	B(E2) (e^2fm^4) ASDI [c]
1.08	→	0	2_1^+	→	0_1^+	272 ± 12 [d]	270 ± 40
1.66	→	1.08	0_2^+	→	2_1^+		29 ± 4
1.88	→	0	2_2^+	→	0_1^+	8.8 ± 1.6 [d]	8 ± 5
	→	1.08		→	2_1^+	270 ± 50 [e]	350 ± 50
	→	1.66		→	0_2^+	150 ± 30 [e]	1.2 ± 0.4
2.34	→	1.08	2_3^+	→	2_1^+		10 ± 3
	→	1.88		→	2_2^+		22 ± 3
(2.42)	→	1.08	4_1^+	→	2_1^+		280 ± 40
	→	1.88		→	2_2^+		9.4 ± 1.3
(2.96)	→	1.08	4_2^+	→	2_1^+		23 ± 7
	→	1.88		→	2_2^+		104 ± 16
4.16*	→	(2.42)	6_1^+	→	4_1^+		240 ± 40
	→	(2.96)		→	4_2^+		7 ± 3
4.49*	→	(2.42)	6_2^+	→	4_1^+		37 ± 5
	→	(2.96)		→	4_2^+		8.9 ± 1.4

a) Excitation energies are taken from ref. [33]. The conventions of the presentation are explained under footnote a) in table 4a.

b) See caption of table 4a.

c) Radial wave functions as in table 4a but with effective charges of 2.0 ± 0.2 and 1.0 ± 0.1 for the proton and neutron, respectively. The single-particle estimate corresponds to a B(E2) value of 16 e^2fm^4.

d) From (e,e') experiment of ref. [50].

e) Calculated from branching and mixing ratios of ref. [33] and the deduced mean life of τ_m=2.3±0.4 ps for the 2_2^+ state from ref. [50].

TABLE 5

A comparison of calculated B(E2) and B(M1) values with experiment

Nucleus	$E_{xi} \rightarrow E_{xf}$ [a] (MeV)	$J_i^\pi \rightarrow J_f^\pi$ [b]	B(E2) (e^2fm^4) Expt.	B(E2) QPC [c]	B(E2) ASDI [d]	100 × B(M1) (μ_N^2) Expt. [c]	100 × B(M1) ASDI f)	100 × B(M1) ASDI g)
^{62}Zn	1.80 → 0.95	$2_2^+ \rightarrow 2_1^+$			- 70 ±11		0.7	0.3
^{63}Zn	0.19 → 0	$5/2_1^- \rightarrow 3/2_1^-$	> 81 [h]		76 ±12	>0.3 [h]	0.2	0.03
	(0.64) → 0	$3/2_2^- \rightarrow 3/2_1^-$			- 5.1± 0.9		-28	-7
^{64}Zn	1.80 → 0.99	$2_2^+ \rightarrow 2_1^+$	560±50 [i]		160 ±20	≈0.3 [i]	- 2.5	-1.2
^{65}Zn	0.05 → 0	$1/2_2^- \rightarrow 5/2_1^-$	103±6 [h]		98 ± 2			
	0.12 → 0	$3/2_1^- \rightarrow 5/2_1^-$	240±140 [j]		- 0.4± 0.1	4.5±0.5 [j]	-1.3	-0.5
	→0.05	$\rightarrow 1/2_2^-$	<1000 [j]		- 41 ± 7	>6.8 [j]	3.7	4.8
	0.21 → 0	$3/2_2^- \rightarrow 5/2_1^-$	160±100 [j]		-410 ±80	-0.5 [j]	0.2	0.3
	→0.05	$\rightarrow 1/2_2^-$	450±250 [j]		6.6± 1.5	-5.4 [j]	-13	-2.9
	0.77 → 0	$5/2_2^- \rightarrow 5/2_1^-$			-13 ± 2		- 2.1	-0.3
	0.86 → 0	$7/2_1^- \rightarrow 5/2_1^-$			-260 ±40		0.8	0.4
^{66}Zn	1.87 → 1.04	$2_2^+ \rightarrow 2_1^+$	≈7×10^3 [k]		260 ±40	≈4 [k]	-11	-8.2

TABLE 5 Continued.

Nucleus	$E_{xi} \rightarrow E_{xf}$ [a] (MeV)	$J_i^\pi \rightarrow J_f^\pi$ [b]	B(E2) (e^2fm^4) Expt.	B(E2) QPC [c]	B(E2) ASDI [d]	100 × B(M1) (μ_N^2) Expt. [e]	100 × B(M1) ASDI f)	100 × B(M1) ASDI g)
^{67}Zn	0.09 → 0	$1/2_1^- \rightarrow 5/2_1^-$	4.5±0.2 [h]	5.1	10 ± 2			
	0.18 → 0	$3/2_1^- \rightarrow 5/2_1^-$	46 ±37 [j]		- 75 ±12	-0.55±0.02 [h,j]	- 0.08	-0.07
	→0.09	$\rightarrow 1/2_1^-$	220 ±90 [j]		120 ±20	-0.34±0.01 [h,j]	56	28
	0.39 → 0	$3/2_2^- \rightarrow 5/2_1^-$	7.4± 0.5 [l]	6.5	-130 ±20	+1.0 ±0.4 [m]	0.02	≈0
	→0.09	$\rightarrow 1/2_1^-$	290 ±230 [m]	30	0.1± 0.2	-7 ±3 [m]	-37	-23
	0.81 → 0	$7/2_1^- \rightarrow 5/2_1^-$	221 ±15 [l]	482	220 ±40	-0.07±0.02 [m]	- 0.4	- 0.4
	(0.87) → 0	$3/2_3^- \rightarrow 5/2_1^-$	600 ±300 [l]	92	49 ±12		0.01	0.03
	0.89 → 0	$5/2_2^- \rightarrow 5/2_1^-$	86 ± 6 [l]	307	- 98 ±15	-2.1 ±1.8 [m]	0.5	0.6
	(1.52) → 0	$9/2_1^- \rightarrow 5/2_1^-$			-170 ±30			
^{68}Zn	1.88 → 1.08	$2_2^+ \rightarrow 2_1^+$	270 ±50 [n]		270 ±40	-1.4 ±0.3 [n]	-25	-26

[a] Excitation energies are taken from refs.[27-33]. Values enclosed in parentheses indicate the lack of a firm experimental spin-parity assignment.

[b] Lower indices denote the number of the eigenvector used in the calculation.

[c] From a quasiparticle-phonon coupling calculation of ref.[5]

[d] From the present calculation with harmonic-oscillator wave functions with $\hbar\omega = 41A^{-1/3}$ for the radial part of the used single-particle matrix elements and effective charges of e_p=1.6±0.2 and e_n=1.0±0.1 for proton and neutron, respectively. The sign of the B(E2) value corresponds to the sign of the transition matrix element.

TABLE 5 Continued.

e) The sign of the B(M1) value corresponds to the sign of the experimental mixing ratio.

f) From the present calculation with bare-nucleon g-factors for the reduced single-particle M1 matrix elements. The sign of the B(M1) value corresponds to the sign of the transition matrix element.

g) Similar to f) but now with effective reduced single-particle matrix elements, see text.

h) From ref.[53].

i) Deduced from refs.[50,51].

j) From refs.[30,32,54].

k) Deduced from refs.[31,52].

l) From ref.[5].

m) Deduced from B(E2) values of ref.[5] and mixing and branching ratios of ref.[32].

n) Deduced from values of refs.[33,50].

TABLE 6

A Comparison of calculated and experimental quadrupole and dipole moments.

Nucleus	E_x (MeV)	J^π	Q2 ($e\,fm^2$) Expt.	Q2 MFB c)	Q2 MFB d)	Q2 ASDI e)	Q2 ASDI f)	MM (μ_N) Expt.	MM ASDI g)	MM ASDI h)
^{62}Zn	0.95	2_1^+		+60		$-33^{\pm 3}$	-41		+1.05	+0.92
	1.80	2_2^+				$+30^{\pm 3}$	+37		+0.33	+0.40
^{63}Zn	0	$3/2_1^-$	+31[a]	-68		$+23^{\pm 2}$	+32	-0.282[a]	-0.71	-0.29
	0.19	$5/2_1^-$				$-10^{\pm 1}$	-15		+1.49	+0.86
^{64}Zn	0.99	2_1^+	$-13.5^{\pm 1.6}$[b]	+58	-13	$-29^{\pm 3}$	-35		+1.12	+0.99
	1.80	2_2^+				$+23^{\pm 2}$	+30		+0.59	+0.65
^{65}Zn	0	$5/2_1^-$	-2.6[a]		0	$-1.1^{\pm 0.1}$	-2.7	+0.769[a]	+1.43	+0.82
	0.12	$3/2_1^-$				$+22^{\pm 2}$	+31	$-0.71^{\pm 0.18}$[i]	-1.06	-0.48
	0.21	$3/2_2^-$				$+12^{\pm 1}$	+14	$+0.66^{\pm 0.23}$[i]	+0.52	+0.29
^{66}Zn	1.04	2_1^+		+45	-12	$-19^{\pm 2}$	-18		+1.29	+1.16
	1.87	2_2^+				$+16^{\pm 2}$	+17		+0.71	+0.74
^{67}Zn	0	$5/2_1^-$	+17[a]	+ 8	+ 6	$+9.8^{\pm 0.8}$	+14	+0.8754[a]	+1.47	+0,85
	0.09	$1/2_1^-$						$+0.58^{\pm 0.03}$[i]	+0.66	+0.58
	0.18	$3/2_1^-$				$-0.6^{\pm 0.2}$	+0.6	$+0.45^{\pm 0.06}$[i]	-0.26	-0.12
^{68}Zn	1.08	2_1^+		+34	-8.8	$-6.2^{\pm 1.7}$	+4.4		+1.51	+1.37
	1.88	2_2^+				$+5.2^{\pm 0.8}$	+2.2		+0.93	+0.85

TABLE 7

A comparison between calculated and experimental log ft values for allowed beta decay

	$J_i^{\pi a)}$		$J_f^{\pi a)}$	E_{xf}(Mev)[b]	log ft		
					Expt.[c]	ASDI[d]	
^{63}Ga	$(3/2_1^-)$	^{63}Zn	$3/2_1^-$	0	5.0	5.1	
			$5/2_1^-$	0.19	6.0	7.6	
			$1/2_1^-$	(0.25)	6.2	5.4	
			$3/2_4^-$	(1.07)	5.8	6.2	
^{64}Ga	0_1^+	^{64}Zn	1_1^+	3.19	5.0	4.9	
			1_3^+	3.37	4.9	4.9	
^{65}Ga	$3/2_1^-$	^{65}Zn	$5/2_1^-$	0	$\geq$6.5	6.2	
			$1/2_2^-$	0.05	5.8±0.2	4.8	
			$3/2_1^-$	0.12	5.0	4.7	
			$3/2_2^-$	0.21	5.6±0.1	5.6	
			$5/2_2^-$	0.77	5.8	5.0	
^{66}Ga	0_1^+	^{66}Zn	1_1^+	(3.23)	6.1	5.0	
			1_2^+	(3.38)	6.5	6.2	
^{67}Ga	$3/2_1^-$	^{67}Zn	$5/2_1^-$	0	$\geq$6.4	5.4	
			$1/2_1^-$	0.09	5.3	4.7	
			$3/2_1^-$	0.18	5.5	5.1	
			$3/2_2^-$	0.39	5.2	5.2	
			$5/2_2^-$	0.89	5.6	7.8	

a) From ref. 55).

b) From ref. 2).

c) Values calculated with Hartree-Fock-Bogoliubov (HFB) wave functions in a full 0f-1p configuration space, employing a Kuo-Brown interaction, but without projection as reported in ref. 9). Effective charges of 1.8 and 0.8 have been used for proton and neutron, respectively.

d) Values calculated with HFB in a full 0f-1p configuration space, employing a Yukawa-Rosenfeld interaction but with projection of good angular momentum 8). Also here effective charges of 1.8 and 0.8 have been used.

e) From present calculations with harmonic oscillator-single-particle wave functions with $\hbar\omega = 41A^{-1/3}$ and effective charges of $1.6^{+}_{-}0.2$ and $1.0^{+}_{-}0.1$ for proton and neutron, respectively.

f) Similar to e) but with effective charges of 1.1 and 2.1 for proton and neutron, respectively.

g) From present calculations and bare-nucleon g-factors.

h) From present calculations and effective reduced single-particle matrix elements, see text.

i) From ref. 54).

TABLE 7 Continued

	$J_i^{\pi a)}$		$J_f^{\pi a)}$	E_{xf}(MeV) b)	log ft	
					Expt. c)	ASD1 d)
^{68}Ga	1_1^+	^{68}Zn	0_1^+	0	5.2	6.2
			2_1^+	1.08	5.5	5.1
			2_2^+	1.88	5.9	4.9

a) Lower indices denote the eigenvector used in the calculation.

b) Excitation energies have been taken from refs. [28-33]. Values enclosed in parentheses indicate the lack of a firm experimental spin-parity assignment.

c) Log ft values for this sequence of Zn isotopes have been taken from ref. [28], ref. [25], refs. [59,60], ref. [31], ref. [32], and ref. [33], respectively. If no errors are quoted, the uncertainty is smaller than the last digit. For the other cases average values of the quoted refs. and the external errors have been used.

d) Calculated with the present wave functions and a value of 1.53 for the square of the ratio of Gamow-Teller to Fermi coupling constants.

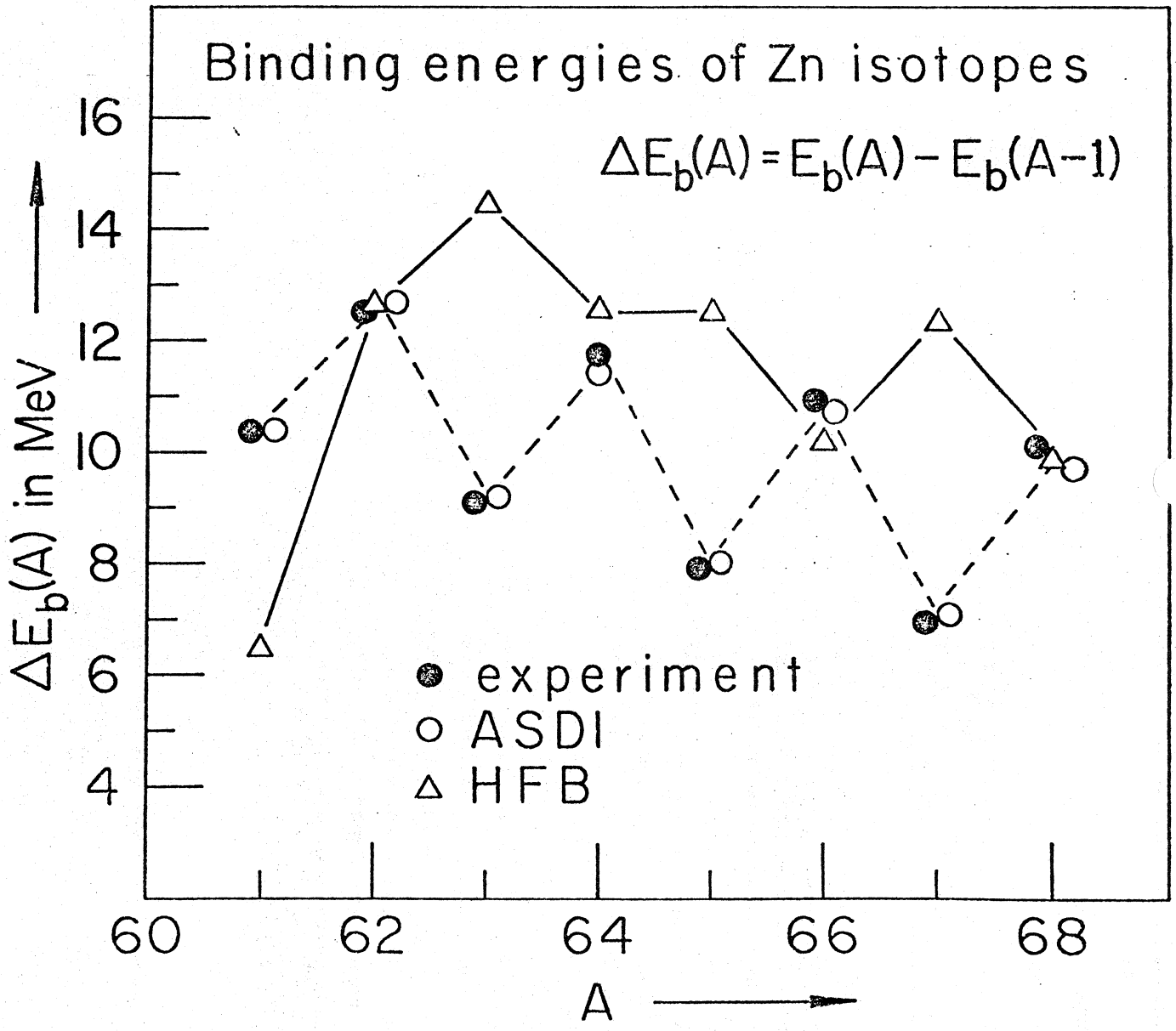
Binding energies of Zn isotopes
$\Delta E_b(A) = E_b(A) - E_b(A-1)$
$\Delta E_b(A)$ in MeV
16
14
12
10
8
6
4
experiment
ASDI
HFB
60
62
64
66
68
A

fig.1

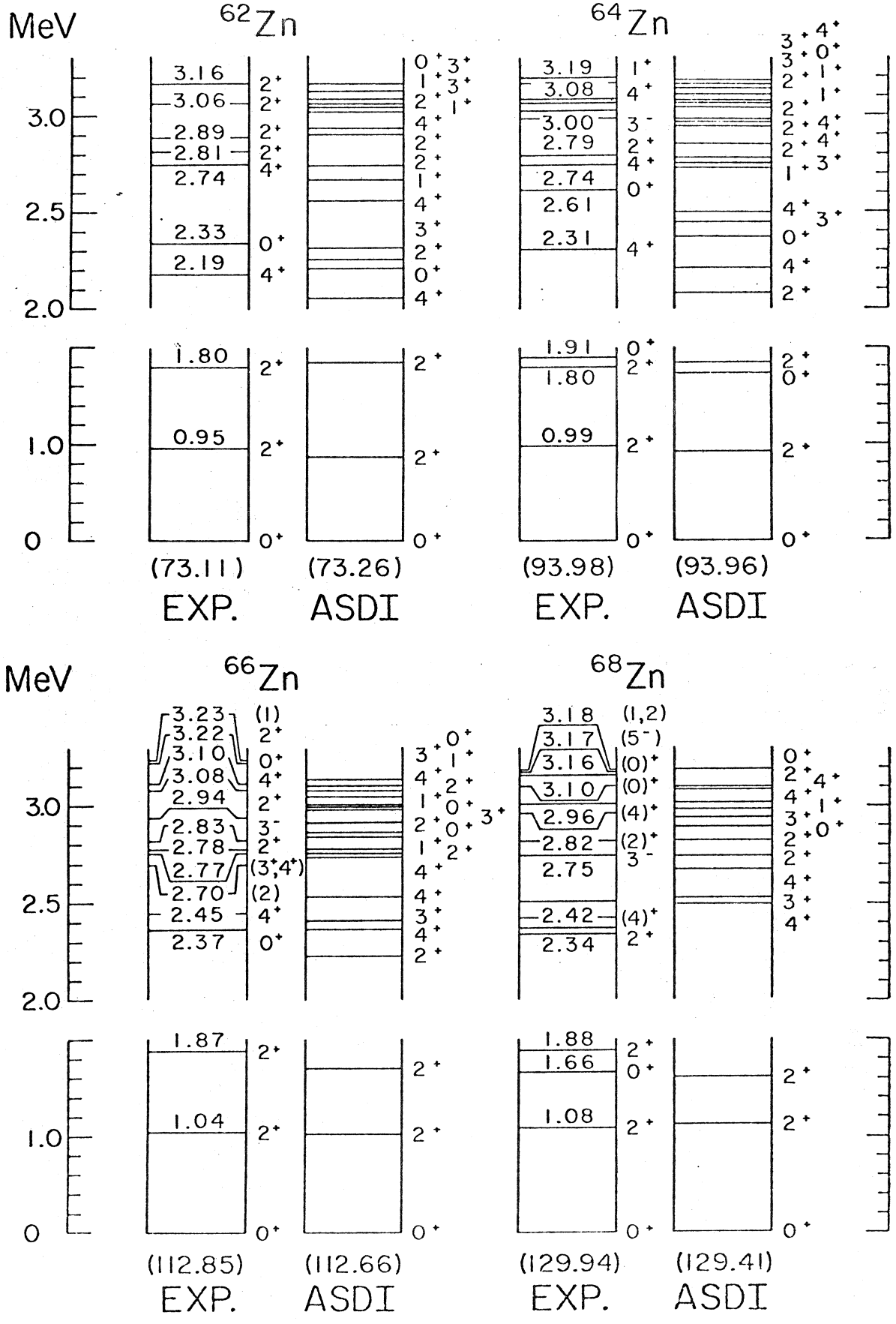
MeV
62Zn
64Zn
3.0
2.5
2.0
1.0
0
3.16
3.06
2.89
2.81
2.74
2.33
2.19
1.80
0.95
3.19
3.08
3.00
2.79
2.74
2.61
2.31
1.91
1.80
0.99
(73.11)
(73.26)
(93.98)
(93.96)
EXP.
ASDI
EXP.
ASDI
MeV
66Zn
68Zn
3.23
3.22
3.10
3.08
2.94
2.83
2.78
2.77
2.70
2.45
2.37
1.87
1.04
3.18
3.17
3.16
3.10
2.96
2.82
2.75
2.42
2.34
1.88
1.66
1.08
(112.85)
(112.66)
(129.94)
(129.41)
EXP.
ASDI
EXP.
ASDI

fig.2

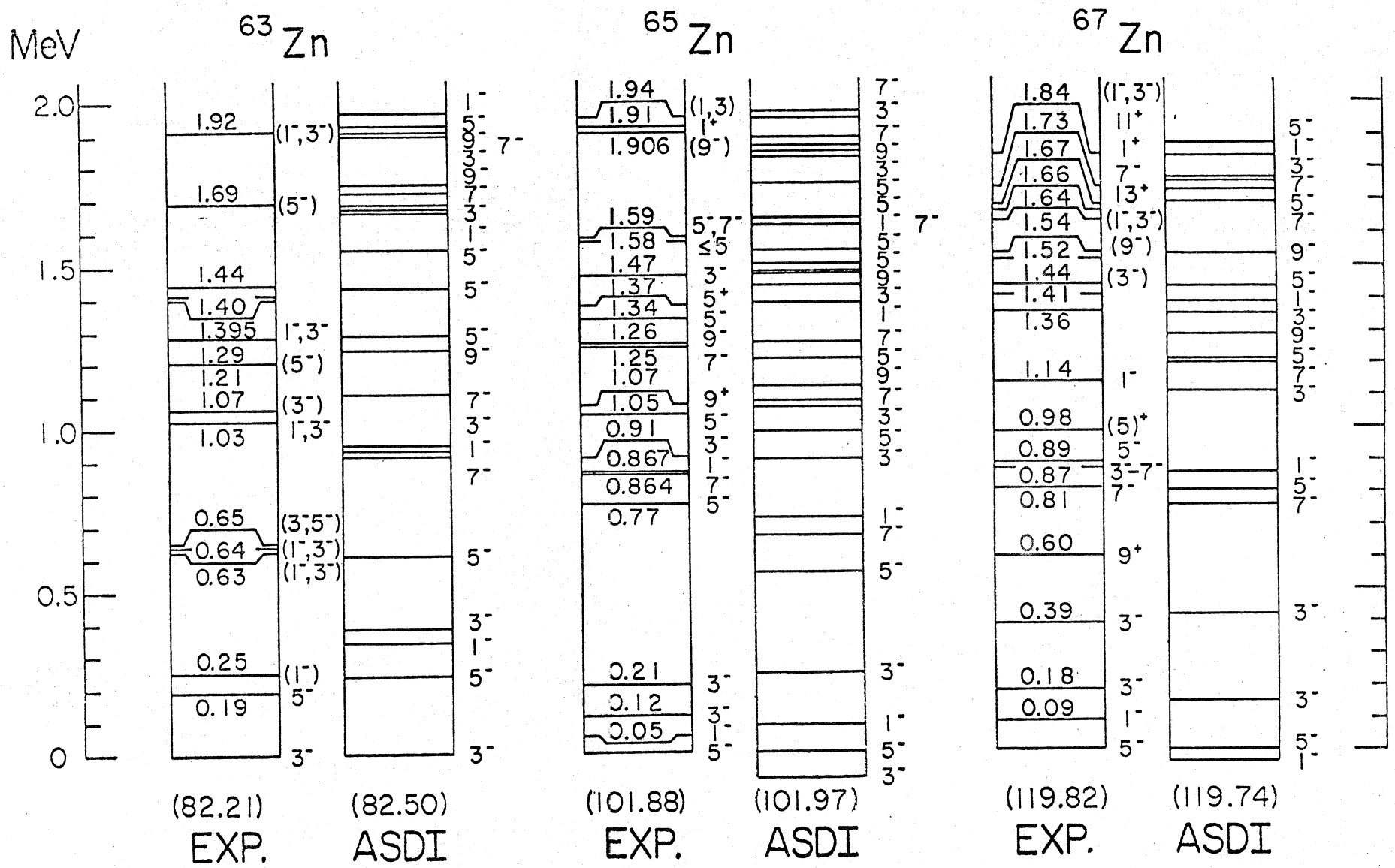
MeV
2.0
1.5
1.0
0.5
0
^{63}Zn
1.92 (1⁻,3⁻)
1.69 (5⁻)
1.44
1.40
1.395 1⁻,3⁻
1.29 (5⁻)
1.21
1.07 (3⁻)
1.03 1⁻,3⁻
0.65 (3,5⁻)
0.64 (1⁻,3⁻)
0.63 (1⁻,3⁻)
0.25 (1⁻)
0.19 5⁻
3⁻
(82.21)
EXP.
(82.50)
ASDI
^{65}Zn
1.94 (1,3)
1.91 1⁺
1.906 (9⁻)
1.59 5⁻,7⁻
1.58 ≤5
1.47 3⁻
1.37 5⁺
1.34 5⁻
1.26 9⁻
1.25 7⁻
1.07
1.05 9⁺
0.91 5⁻
0.867 3⁻
0.864 1⁻
0.77 7⁻
0.21 5⁻
0.12 3⁻
0.05 1⁻
5⁻
(101.88)
EXP.
(101.97)
ASDI
^{67}Zn
1.84 (1⁻,3⁻)
1.73 11⁺
1.67 1⁺
1.66 7⁻
1.64 13⁺
1.54 (1⁻,3⁻)
1.52 (9⁻)
1.44 (3⁻)
1.41
1.36
1.14 1⁻
0.98 (5)⁺
0.89 5⁻
0.87 3⁻-7⁻
0.81 7⁻
0.60 9⁺
0.39 3⁻
0.18 3⁻
0.09 1⁻
5⁻
(119.82)
EXP.
(119.74)
ASDI

fig. 3

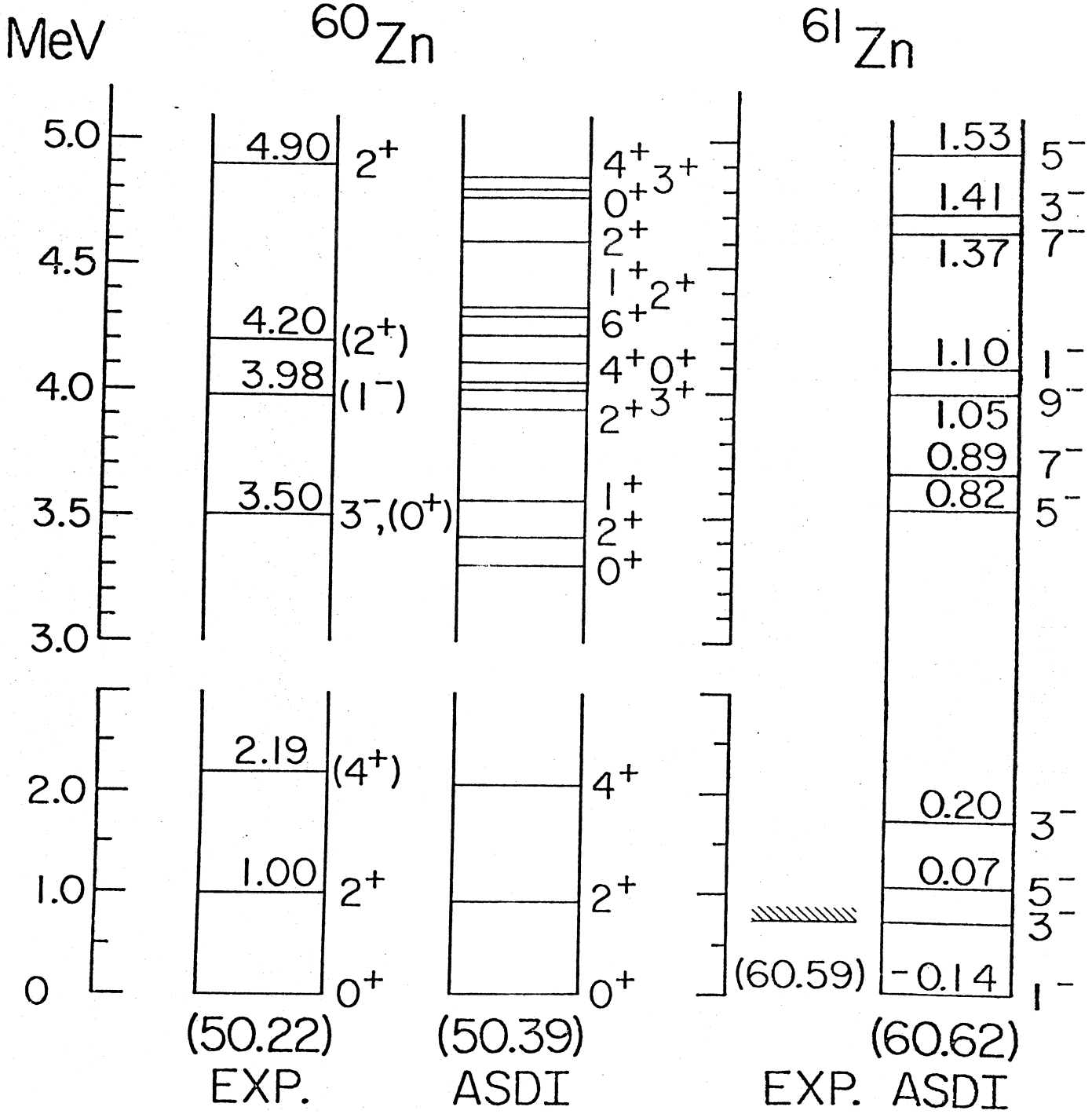
MeV
60Zn
61Zn
5.0
4.5
4.0
3.5
3.0
2.0
1.0
0
4.90 2+
4.20 (2+)
3.98 (1−)
3.50 3−,(0+)
2.19 (4+)
1.00 2+
0+
4+ 3+
0+
2+
1+ 2+
6+
4+ 0+
2+ 3+
1+
2+
0+
4+
2+
0+
(60.59)
1.53 5−
1.41 3−
1.37 7−
1.10 1−
1.05 9−
0.89 7−
0.82 5−
0.20 3−
0.07 5−
3−
-0.14 1−
(50.22)
EXP.
(50.39)
ASDI
(60.62)
EXP. ASDI

fig. 4

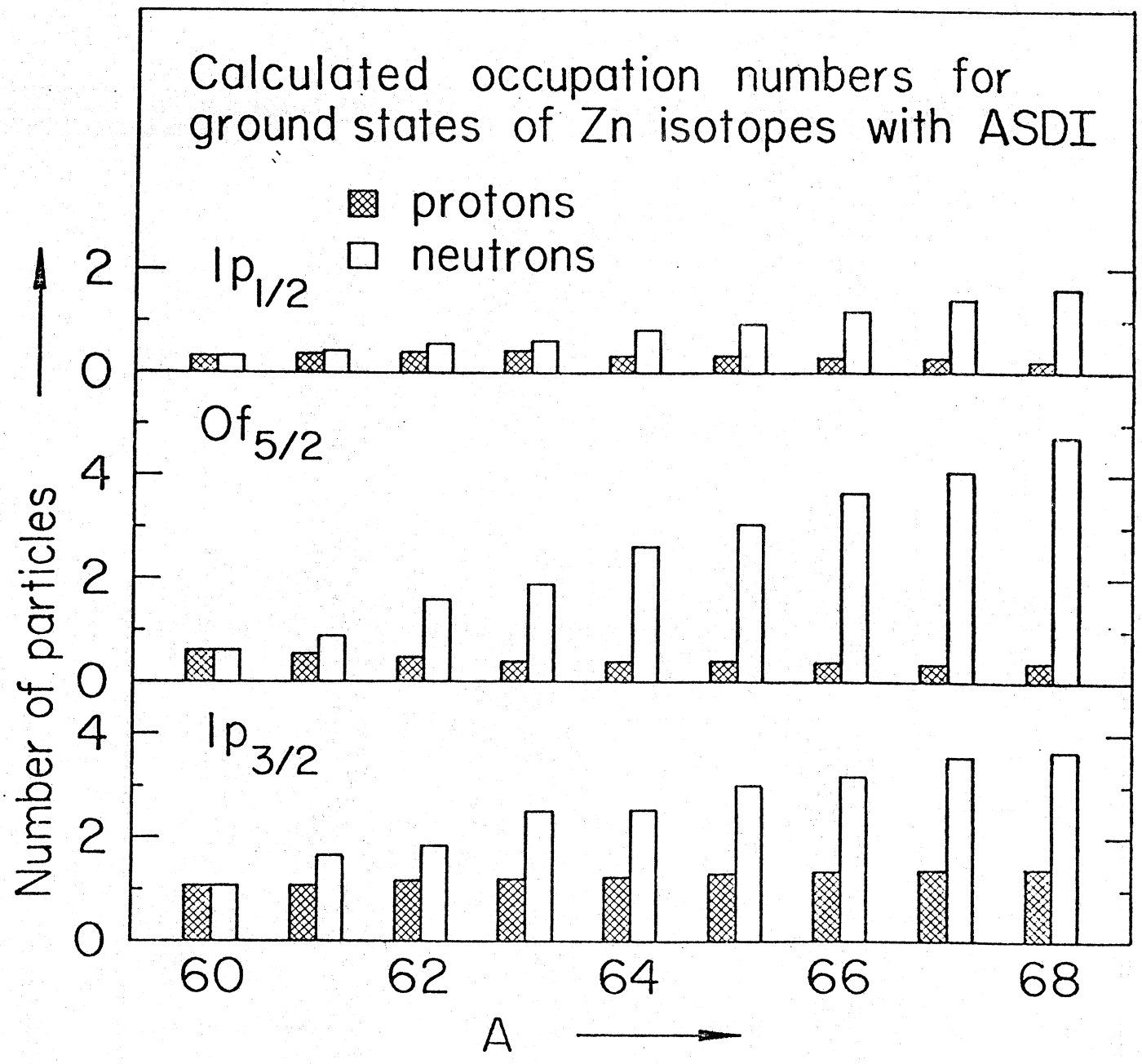
Calculated occupation numbers for ground states of Zn isotopes with ASDI
protons
neutrons
$1p_{1/2}$
$0f_{5/2}$
$1p_{3/2}$
Number of particles
0
2
4
60
62
64
66
68
A

fig.5

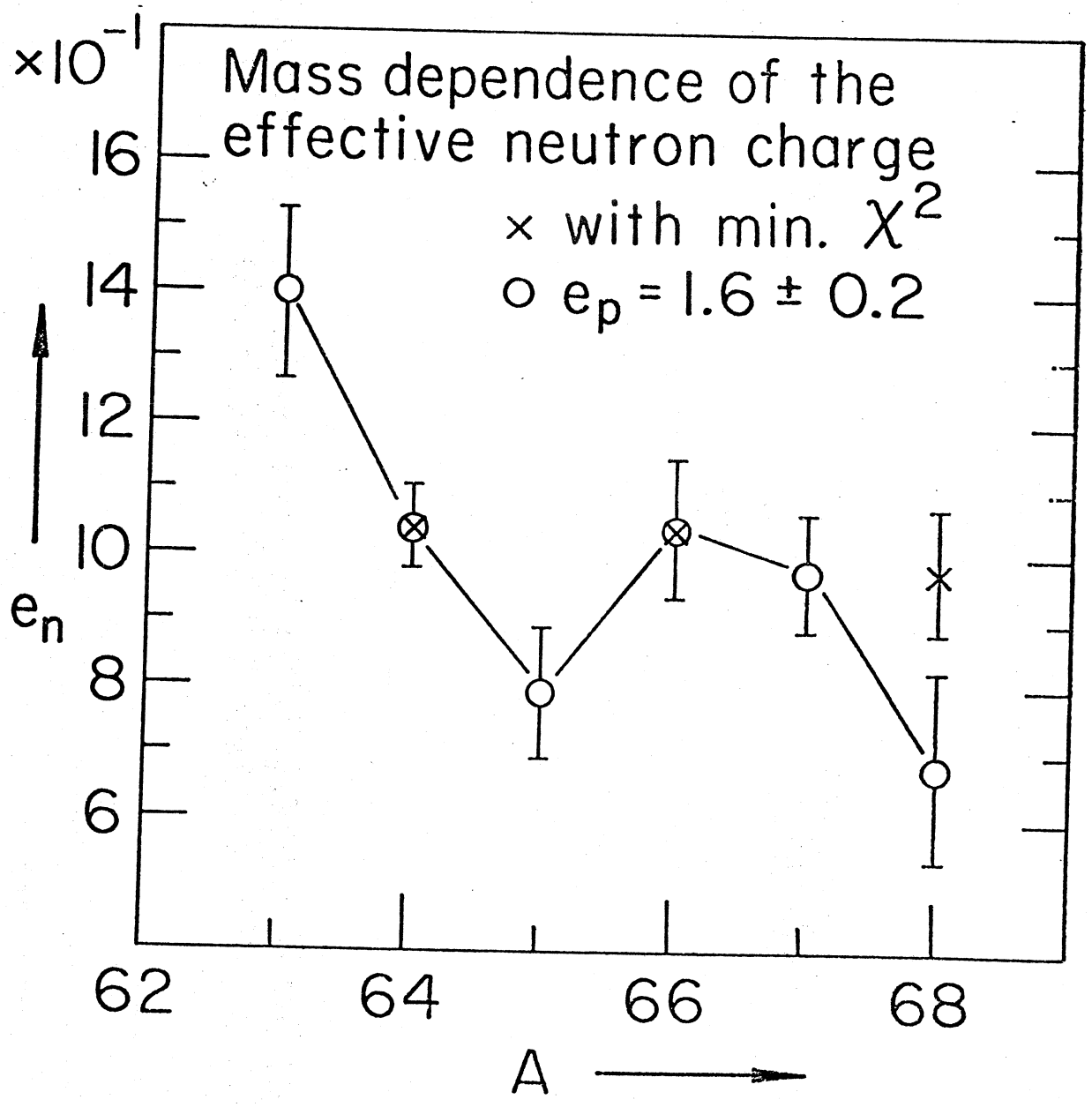
Mass dependence of the
effective neutron charge
× with min. χ^2
○ $e_p = 1.6 \pm 0.2$
$\times 10^{-1}$
16
14
12
10
8
6
e_n
62
64
66
68
A

fig.6